

MOLECULAR LASER STUDY
THREE to FIVE MICRONS

AD729693

Reproduced by
**NATIONAL TECHNICAL
INFORMATION SERVICE**
Springfield, Va. 22151

IBM

**MOLECULAR LASER STUDY
THREE to FIVE MICRONS**

Final Report

Prepared by
Bernard G. Huth
Principal Investigator
IBM
Federal Systems Division
18100 Frederick Pike
Gaithersburg, Maryland 20760

Contract No. N00014-71-C-0010

Sponsored by

ADVANCED RESEARCH PROJECTS AGENCY

ARPA Order No. 306

Program Code. No. 421

Effective Date: August 1, 1970

Expiration Date: July 31, 1971

\$49,980

Scientific Officer: Director, Physics Programs
Physical Sciences Division
Office of Naval Research
Department of the Navy
Arlington, Virginia 22217

DDC
RECORDED
SEP 21 1971
RELEASER
C

The views and conclusions contained in this document are those of the authors and should not be interpreted as necessarily representing the official policies, either expressed or implied, of the Advanced Research Projects Agency or the U. S. Government.

DISTRIBUTION STATEMENT A
Approved for public release;
Distribution Unlimited

FOREWORD

This final technical report covers work performed on a Molecular Laser Research Program, three to five Micron Range, under Contract N00014-71-C-0010. Work on the 12 month program began August 1, 1970, and was carried out at the Federal Systems Division of the International Business Machines Corporation, 18100 Frederick Pike, Gaithersburg, Maryland, 20760.

Dr. F. T. Byrne, Manager of the Laser Physics Department, was the program manager. Dr. Carl F. Shelton was the principal investigator during the first quarter, and Dr. Bernard G. Huth was the principal investigator for the remaining three quarters. Mr. Larry M. Taylor was responsible for portions of the experimental work.

CONTENTS

Section	Page
1 INTRODUCTION	1
2 BRIEF REVIEW OF CO ₂ LASERS	2
2.1 Operation of the Plasma Tubes With CO ₂	3
3 STIMULATED EMISSION FROM ACETYLENE	10
3.1 H ₂ - C ₂ - He Laser Characteristics	10
3.2 Identification of Laser Transition	11
3.3 Possible Pumping Mechanisms	26
3.4 Attempts to Obtain 4 micron Emission	42
4 OTHER GASES	46
5 SUMMARY	54
REFERENCES	56

ILLUSTRATIONS

Figure		Page
1	Pulsed Excitation Plasma Tube With Coaxial Kovar Electrodes	5
2	Typical Operation of the Coaxial-Electrode Tube With Flowing N ₂ - CO ₂ - He	6
3	The Parallel Plasma Tube	7
4	Pulsed Parallel Tube	8
5	Pulsed N ₂ - CO ₂ - He in Parallel Tube	9
6	First Laser Output Obtained From H ₂ - C ₂ H ₂ - He Mixture	12
7	Laser Emission Using Narrow Band Dielectric Mirrors	13
8	Normal Vibrational Modes of Acetylene	14
9	Vibrational Energy Level Diagram of Acetylene	15
10	The Output Spectra of the Acetylene Laser	21
11	Intracavity Absorption Apparatus	23
12	Intracavity Absorption Experiment	24
13	Acetylene Absorption in Extracavity Cell	25
14	$\langle \sigma v \rangle$ vs. Electron Temperature	28
15	Electron Temperature vs. Pressure in Pure Gases	30
16	Operation of the Acetylene Laser Without Hydrogen	31
17	Effect of Hydrogen on the Acetylene Laser Output	34
18	Intensity of a CH Band With and Without Hydrogen	35

Figure		Page
19	Intensity of a C ₂ Swan Band With and Without Hydrogen	36
20	Intensity of a CH Band With and Without Nitrogen	37
21	Plasma Tube Designed to Reduce Unexcited Gas	44
22	Vibrational Energy Level Diagram of Ammonia	47
23	Vibrational Energy Level Diagram of Methane	49
24	Vibrational Energy Level Diagram of Water Vapor	52

TABLES

Number		Page
1	Q-Branch Lines of the $\nu_2 - \nu'_5$ Band of C_2H_2 Calculated from Herzberg's Data	18
2	Q-Branch Lines of the $\nu_2 - \nu'_5$ Band of C_2H_2 Calculated from Keller's Data	20
3	Effects of H_2 and N_2 on the C_2H_2 Laser	33
4	Lifetime by Diffusion to Walls	41
5	Some Infrared Transitions in Acetylene	43
6	Possible Vibrational Transitions in Ammonia - NH_3	48
7	Possible Vibrational Transitions in Methane - CH_4	50
8	Possible Vibrational Transitions in Water	53

Section 1. INTRODUCTION

Laser emission at 8.03 microns was discovered at IBM by Dr. C. F. Shelton in a mixture of $H_2-C_2H_2-He$ ⁽¹⁾. Prior to this contract, the laser emission was tentatively identified as a Q-branch line of the $\nu_2 - \nu^{15}$ band of acetylene, although other possible discharge products had not been eliminated from consideration. The particular choice of gases in the laser resulted from a desire to find an analog to the N_2-CO_2-He laser which would employ vibrational energy transfer from the metastable hydrogen molecules in a gas discharge. Use of metastable hydrogen energy levels offered the possibility of a molecular laser in the three to five micron region of the spectrum due to the higher energy of the $H_2^* (v=1)$ level at 4159.2 cm^{-1} compared to that of $N_2^* (v=1)$ at 2330.7 cm^{-1} .

If vibrational energy transfer from H_2^* were instrumental in populating the upper laser state in acetylene, there would be a possibility of finding a number of new laser lines in a very useful portion of the infrared spectrum. Therefore, this research program was undertaken to acquire more knowledge about the acetylene laser and to search for additional laser materials based on these ideas. The program was divided into three tasks:

- a. Study the eight micron emission from $H_2-C_2H_2-He$
- b. Investigate the possibility of obtaining four micron laser emission from $H_2-C_2H_2-He$
- c. Experiment with other gases which have vibrational resonances with molecular hydrogen.

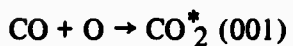
This report is organized as follows: Section 2 contains a brief review of CO_2 lasers and a description of the operation of some of our plasma tubes with flowing mixtures of N_2-CO_2-He ; Section 3 describes the experimental work with acetylene and contains a discussion of the results, including the unsuccessful attempts to obtain four micron emission; Section 4 relates our attempts to achieve laser action in several other gases; and Section 5 is a summary of the results.

Section 2. BRIEF REVIEW OF N₂-CO₂-He LASERS

The pumping mechanisms and operation of the N₂-CO₂-He laser system have been discussed widely in the open literature and thus will only be summarized.

Excitation mechanisms for pumping CO₂ to the upper laser level include:

- a. Direct electron impact⁽²⁾
- b. Vibrational energy transfer⁽³⁾ through inelastic collisions with N₂^{*} (v=1)
- c. Recombinations⁽⁴⁾ of the form



Helium enhances the CO₂ laser output by at least five mechanisms:

- a. Helium depopulates the 01¹0 mode through inelastic collisions and thus indirectly increases the rate of depopulation of the lower laser level, i.e., the 10⁰0 level⁽⁵⁾.
- b. Helium increases the rate of rotational thermalization within each vibrational level and thus maintains the population inversion on the strongest vibrational-rotational transitions.
- c. Helium cools the kinetic temperature of the gas mixture because of its higher thermal conductivity.
- d. Helium shifts the electron temperature and/or the electron density to more favorable values for vibrational excitation by electron impact^(5,6).
- e. Helium reduces the diffusion of the excited species to the walls of the plasma tube where they can be de-excited.

Effect b shows up in the fact that fewer rotational P-branch lines are observed in N_2 - CO_2 -He mixtures than in N_2 - CO_2 mixtures. Patel⁽⁷⁾ observed emission on the P(12) through P(38) lines of the $\nu_3 - \nu_1$ band with pure CO_2 . Other researchers have observed emission on the P(18) through P(28) lines using N_2 - CO_2 ⁽⁸⁾, the P(20) through P(26) lines using CO_2 -He⁽⁹⁾ and the P(20) through P(24) using N_2 - CO_2 -He⁽¹⁰⁾. Since only the even P-branch lines are allowed this means a reduction from 14 lines using pure CO_2 to four lines using CO_2 -He and to three lines using N_2 - CO_2 -He.

The actual effects of He on electron temperature and electron density in the plasma have not been accurately measured during laser emission, however, these effects can be inferred in various ways. Patel⁽¹¹⁾, for example, observed an increase in output from his parallel pumped N_2 - CO_2 laser⁽¹²⁾ with increasing helium partial pressure when the helium was added through the CO_2 port and CO_2 -He mixed with vibrationally excited N_2 in the interaction region. A greater increase in power output, by roughly a factor of two, was observed by Patel when the helium was added through the N_2 port and was thus in the parallel discharge with the N_2 prior to mixing with CO_2 in the interaction region.

The electron-energy distribution in the positive column of a normal glow discharge is controlled in part by the ionization potentials of the components of the gas mixture. The trend is to a higher electron temperature with higher ionization potentials^(5,13). The ionization potentials of N_2 , CO_2 and He are 15.5, 13.79, and 24.58ev, respectively. Typical mixtures used for laser emission vary, but a mixture of 2/1/10, N_2 / CO_2 /He is not uncommon.

Thus, there is some evidence that one of the functions of helium in N_2 - CO_2 -He lasers is to shift the electron temperature to a slightly higher value for a given total pressure and thus increase the pumping of the upper laser level by direct electron impact and by vibrational energy transfer from N_2^* ($v=1$).

2.1 OPERATION OF THE PLASMA TUBES WITH CO_2

Several plasma tubes with internal mirrors were constructed for use with acetylene. The operation of these tubes with flowing mixtures of N_2 - CO_2 -He is given in the following paragraphs as a point-of-reference-for those with CO_2 experience.

The simple plasma tube used for most of the pulsed work is shown in Figure 1. The mirrors are exposed to the vacuum, and are mounted using stainless steel bellows. Operation of the tube with N_2 -CO₂-He is indicated in Figure 2. The ratio of N_2 :CO₂:He used for the data shown was 2:1:4 at 8 Torr and produced pulse energies of 15 to 20 millijoules.

The parallel tube shown in Figure 3 produced CW power outputs in excess of 600mW from CO₂ which had been pumped only from a resonant energy transfer from N₂ which was excited in the parallel discharge. For these experiments, a 95 percent reflectivity dielectric mirror for output coupling and an input power of 220 watts were used. This compares to an output power of 2mW with an input power of 100 watts obtained by Patel(12).

This parallel tube was also operated in the pulsed mode by the addition of two electrodes near the center of the discharge region to prevent the plasma from traveling down the interaction region. Figure 4 shows the modified tube and the pulse circuitry.

A 0-16Kv, 0-12ma dc power supply was used to charge a 0.02uf capacitor. This charge was then applied to the plasma tube after the electrode shown on the right in Figure 4 was switched to ground by the thyratron tube. The pulse repetition rate could be controlled by a pulse generator which triggered the thyratron. Two Welch Model 1397, 15cfm each, mechanical pumps were operated in parallel to continuously flow gas mixtures through the plasma tube. Partial pressures and flow rates of up to three component gases could be controlled through the use of needle valves, flow meters, and a manifold arrangement. Partial pressures were measured upstream of the plasma tube using a capacitor manometer.

Figure 5 shows the performance of the tube with CO₂ under pulsed conditions. Output pulse energies were typically three millijoules, and the peak power was approximately seven watts. The nitrogen flow rate was approximately 60 liters per minute at the tube which produced a flow velocity of 400cm per second in each half of the interaction region. Morgan and Shiff have measured the lifetime of the metastable N₂^{*} (v=1) level at a few Torr to be 114msec, which means that if wall collisions are unimportant, the excited molecules travel 45cm in one decay time⁽¹⁴⁾. Considering both halves of the tube, this represents almost the entire one meter length of the interaction region.

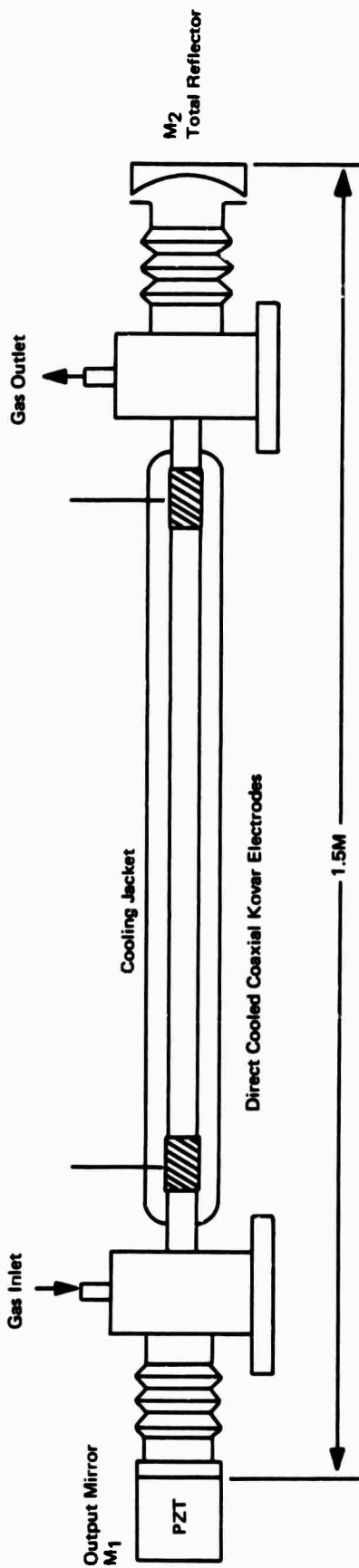


Figure 1. Pulsed Excitation Plasma Tube with Coaxial Kovar Electrodes

AA0800-1

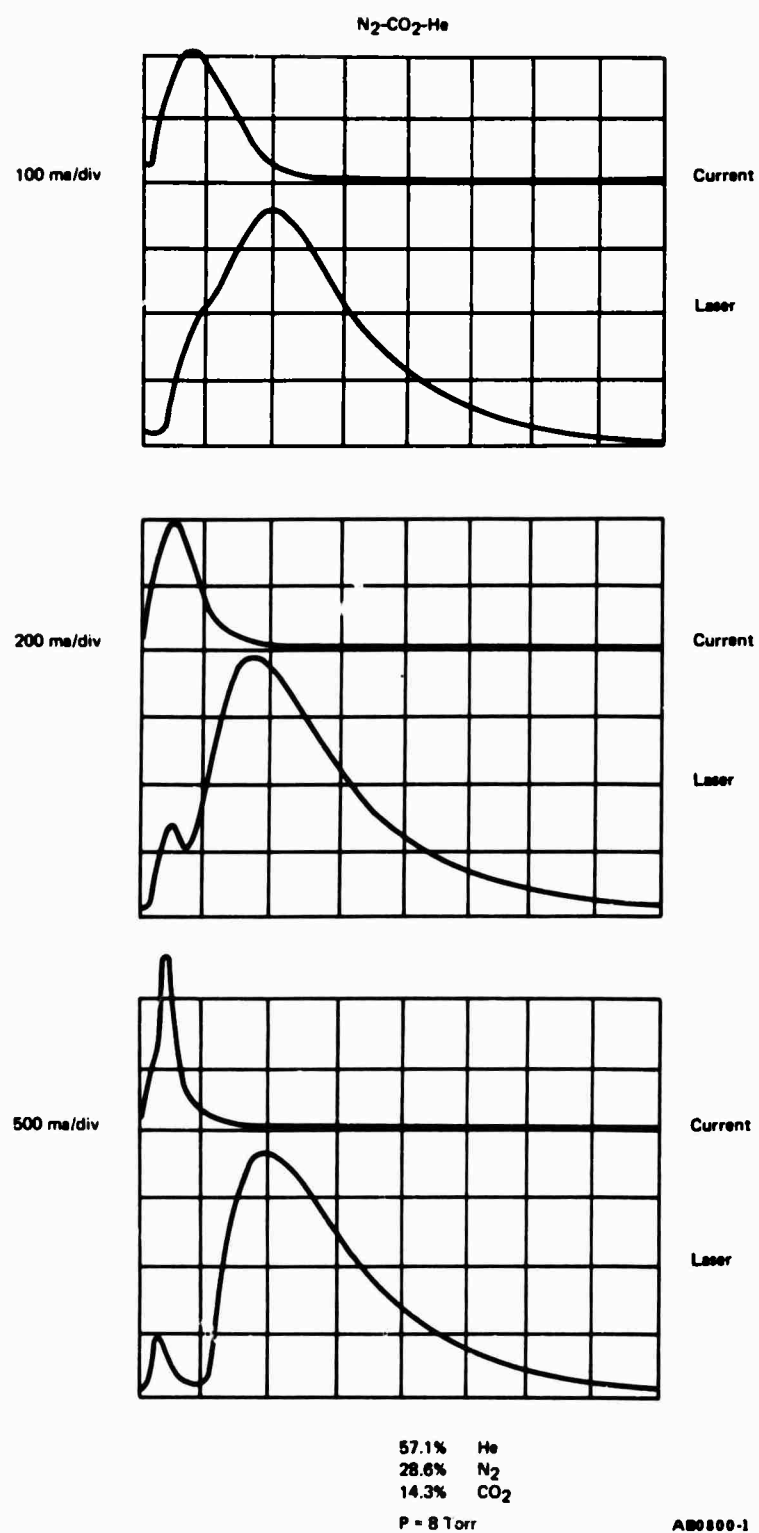
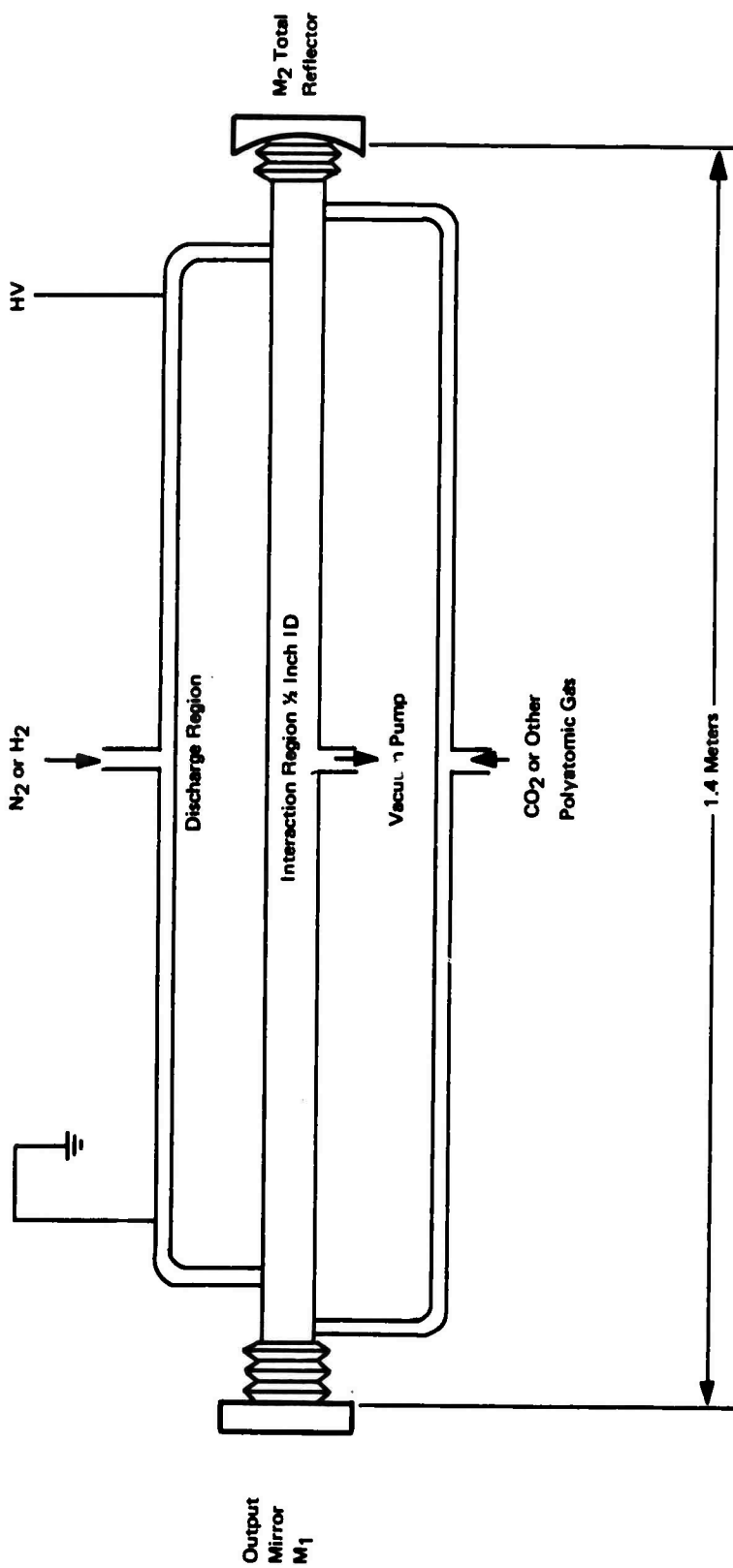


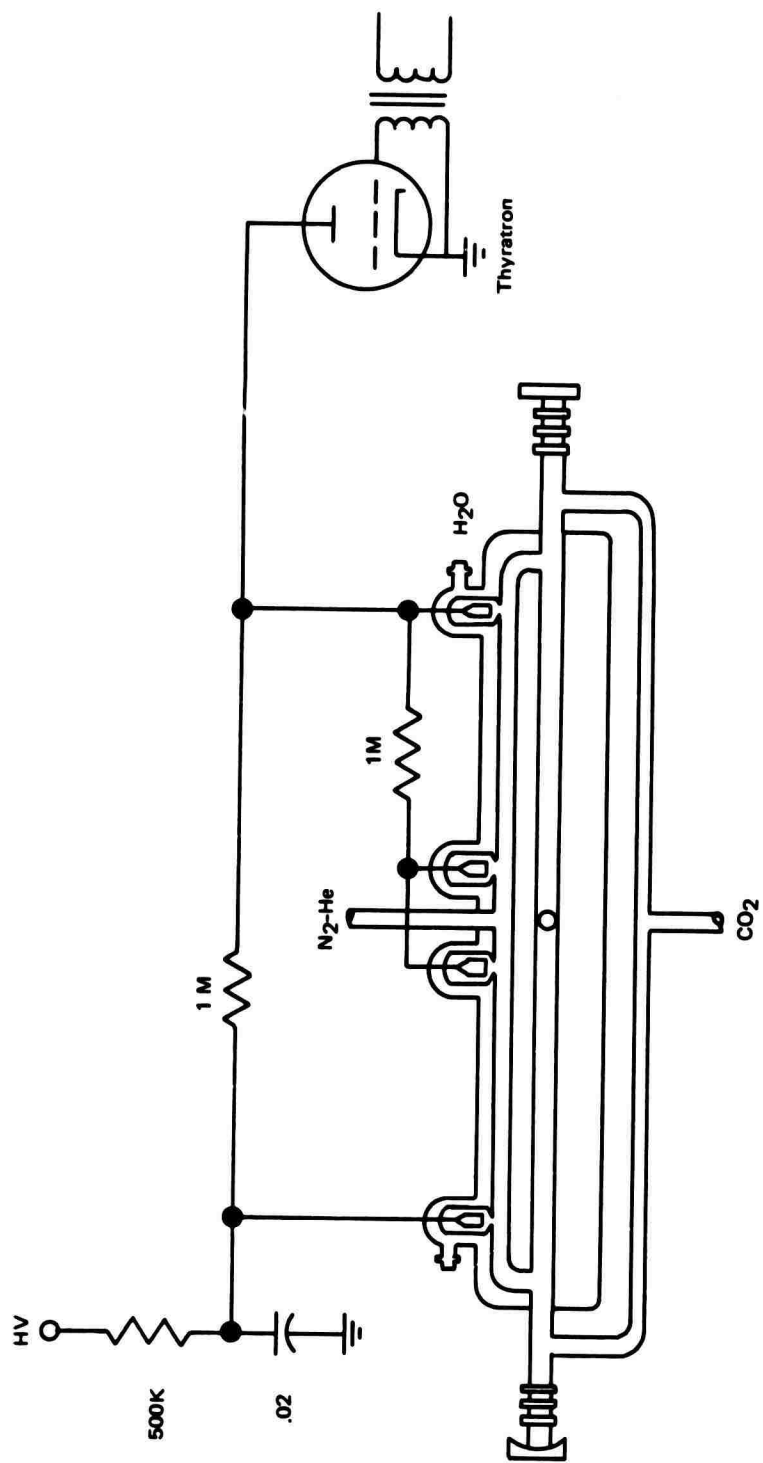
Figure 2. Typical operation of the coaxial-electrode tube with flowing N₂-CO₂-He



The discharge takes place in one of the parallel tubes. Molecules excited by electron impact flow into the interaction region where they can exchange energy with the lasing molecule.

AC0000-1

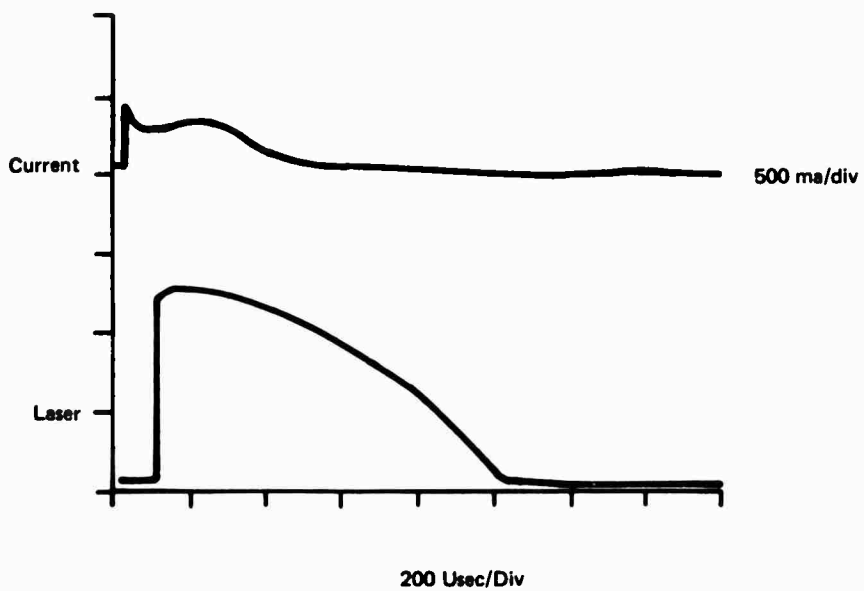
Figure 3. The Parallel Plasma Tube



Additional electrodes have been added to insure that the discharge takes place in the proper portion of the tube.

AD0800-1

Figure 4. Pulsed Parallel Tube



Operation of N₂-CO₂-He in the pulsed parallel tube. N₂ and He were introduced into the discharge end mixed with CO₂ in the interaction region.

AE0800-1

Figure 5. Pulsed N₂-CO₂-He in Parallel Tube

Section 3. STIMULATED EMISSION FROM $H_2\text{-}C_2H_2\text{-}He$

Laser emission near eight microns was obtained from a pulsed discharge in a flowing mixture of $H_2\text{-}C_2H_2\text{-}He$ by Dr. C. F. Shelton.⁽¹⁾ He tentatively identified the transition as a Q-branch line in the $\nu_2 - \nu_1$ band of acetylene. The notion that this laser action may have resulted from vibrational excitation of C_2H_2 via a near resonant energy transfer from the metastable ($v=1$) vibrational level of H_2^* presented interesting possibilities for new infrared lasers. Selective excitation due to the transfer of energy from N_2^* ($v=1$) had been demonstrated in $N_2\text{-}CO_2$, $N_2 - N_2O$, and $N_2 - CS_2$ systems, but no lasers utilizing the metastable state of vibrationally excited H_2 had yet been reported. The higher energy of the H_2^* ($v=1$) level at 4159.2 cm^{-1} compared to that of N_2^* ($v=1$) at 2330.7 cm^{-1} suggested a potentially efficient pumping mechanism for molecular lasers in the three to five micron region of the spectrum.

Most of the effort in the program was directed toward a better understanding of the $H_2\text{-}C_2H_2\text{-}He$ laser since a positive identification of the lasing transition and some indication that vibrational energy transfer existed were both considered of paramount importance in a search for new laser transitions.

Section 3 is subdivided as follows: Subsection 3.1 describes some of the laser characteristics, Subsection 3.2 contains the details of the identification of the transition, Subsection 3.3 discusses possible pumping mechanisms, Subsection 3.4 relates the attempts to obtain four micron emission from acetylene, and, finally, Subsection 3.5 presents a summary and discussion of all the acetylene results.

3.1 $H_2\text{-}C_2H_2\text{-}He$ LASER CHARACTERISTICS

Typical output pulses from the eight micron laser are shown in Figures 6 and 7. In each case, the plasma tube was similar to the one shown in Figure 1. The values of peak power quoted in the figures were measured with no attempt made to optimize the output coupling.

The first laser output observed, as shown in Figure 6, was obtained using an aperture for broadband coupling. The laser emission was usually found to be on a single line at 8.040 microns, and no rotational structure was observed. On one occasion, two lines were observed at 8.034 microns and 8.040 microns.

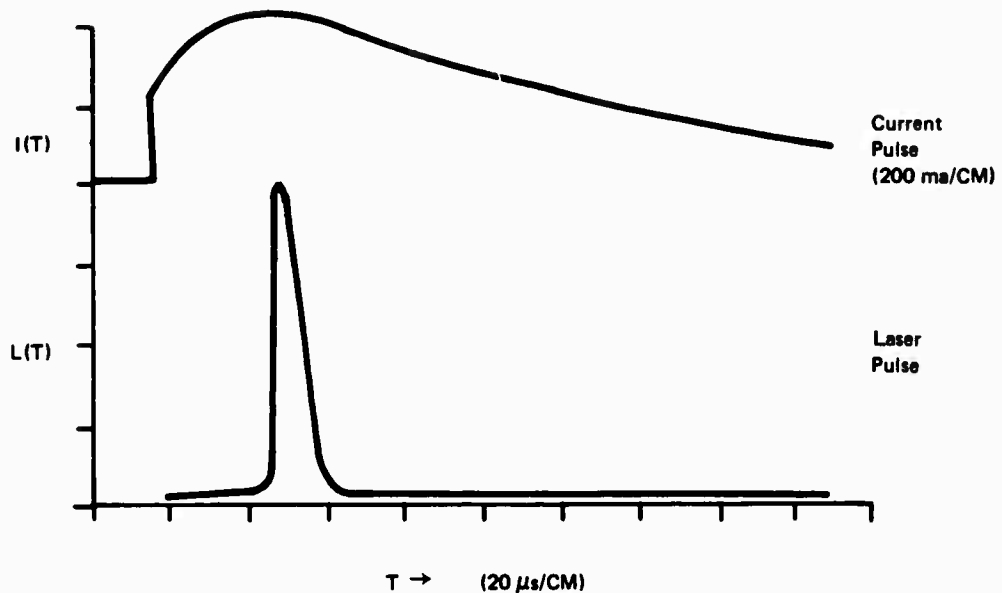
The laser emission obtained using narrow band dielectric mirrors is shown in Figure 7. The pulses shown are for two cooling jacket temperatures. Figure 7b shows the result obtained when the gas mixture was pre-cooled and the cooling jacket temperature was -80°C. The increased laser output at lower temperatures is probably due to a reduced thermal population in the lower lasing state and a reduced Doppler width. Five emission lines were observed at different times under these conditions. The wavelengths in air of these five lines were measured as 8.0313, 8.0329, 8.0352, 8.0383, and 8.0416 microns using the twelfth order of the 6678Å and 6717Å neon lines (at 8.0139 and 8.0605 microns) as a calibration reference. A Jarrell-Ash one-meter Czerny-Turner spectrometer with a 98 groove/millimeter IR grating, blazed at seven microns, was used for the wavelength measurements. This grating gave a linear dispersion of approximately 102Å/mm and a theoretical resolving power of 8Å in the first order. The detector was liquid nitrogen cooled Ge:Au.

The laser emission was obtained at pulse repetition rates from 1 pps up to 250 pps. Power supply limitations, i.e., current capability, prevented operation at higher repetition rates. The discharge ran quite clean, although light carbon deposits were formed near the electrodes after many hours of operation at pulse repetition rates of 26 pps. The side light emission from the plasma was very weak during laser action and could not be observed with the eye when the laboratory lights were turned on.

3.2 IDENTIFICATION OF LASER TRANSITIONS

Acetylene, C_2H_2 is a linear symmetric molecule with five normal modes of vibration.⁽¹⁶⁾ These normal modes are shown in Figure 8. Some of the vibrational energy levels of the ground electronic state of C_2H_2 are shown in Figure 9. In contrast with the $\nu_3 - \nu_1$ band of CO_2 , the $\nu_2 - \nu_1^1$ (01000 - 00001⁰) band of C_2H_2 has an allowed Q-branch.⁽¹⁴⁾ This $\nu_2 - \nu_1^1$ band Q-branch has been observed in absorption by Bell and Nielsen^(17,18) with a Q-branch peak at 1244.5cm^{-1} although the individual Q-branch lines were not resolved by them.

To a first approximation the energy of the Jth rotational level of the ν th vibrational level is given by



M₁: Flat Au-coated BaF₂ with $\frac{1}{8}$ mm dia. hole

M₂: R=5 meters Au-coated

H₂/C₂H₂/He=2/1/20 torr

T_{jacket} = 22°C

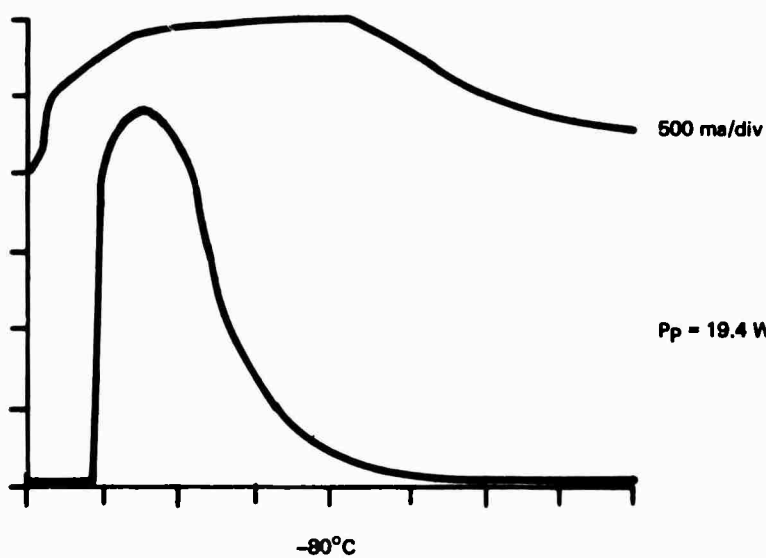
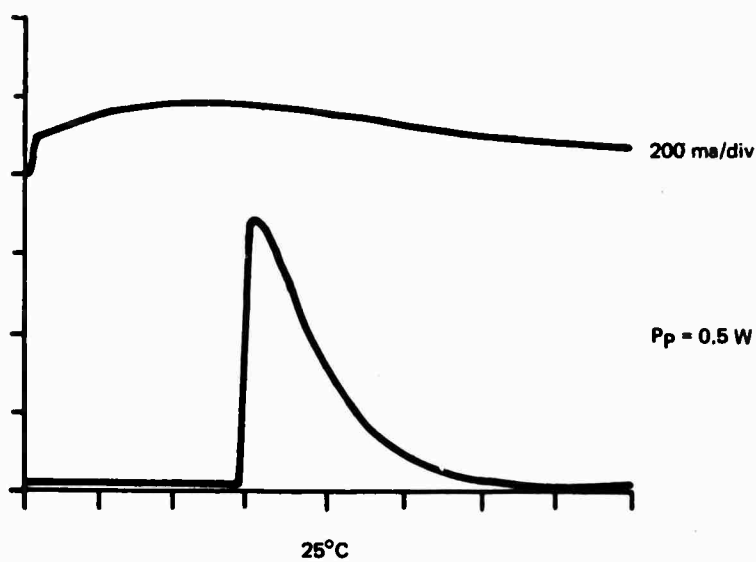
$\frac{1}{8}$ inch ID Plasma tube with neon sign electrodes

Peak power \simeq 5.7 watts

PRF = 32 pulses/sec

AF0800-1

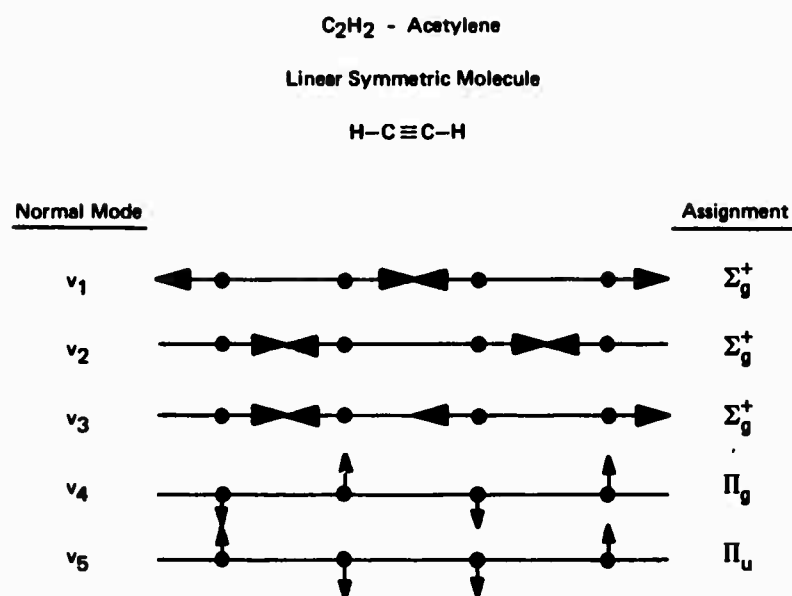
Figure 6. First Laser Output Obtained from H₂-C₂H₂-He Mixture



The effect of reduced temperatures on the 8.03 micron acetylene laser. The ratio of $\text{H}_2:\text{C}_2\text{H}_2:\text{He}$ was 2:1:20 Torr.

AG0800-1

Figure 7. Laser Emission Using Narrow Band Dielectric Mirrors



AH0800-1

Figure 8. Normal Vibrational Modes of Acetylene

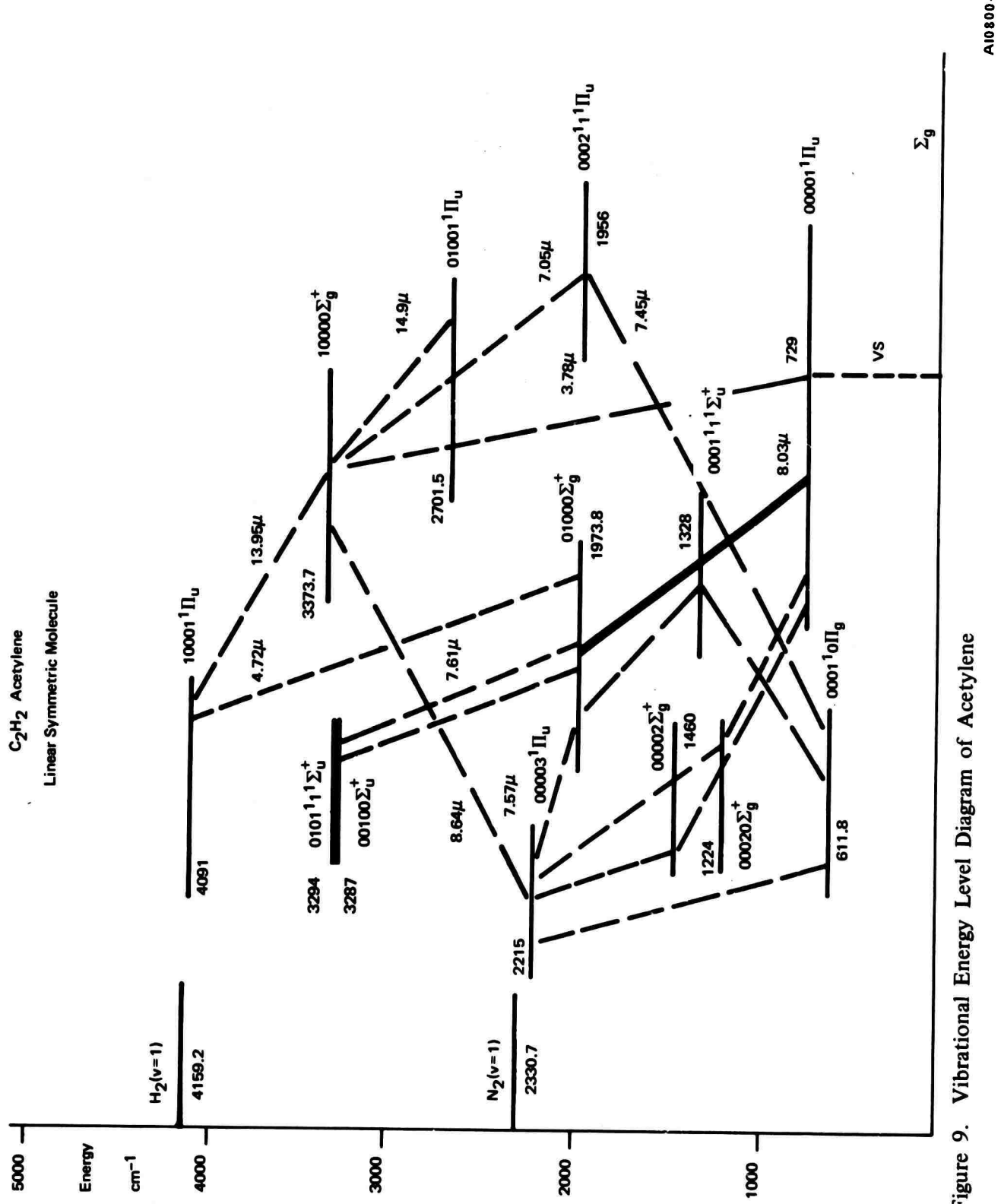


Figure 9. Vibrational Energy Level Diagram of Acetylene

$$E_{\nu, J} = E_{\nu} + B_{\nu} J(J+1) - \ell^2 + \dots \quad (3-1)$$

where $\ell = \ell_4 + \ell_5$ and ℓ_4, ℓ_5 are the angular momentum quantum numbers associated with the two degenerate bending modes ν_4 and ν_5 , respectively. The rotational constant B_{ν} , is given by⁽¹⁶⁾

$$B_{\nu} = B_e - \sum a_i [v_i + d_i/2] \quad (3-2)$$

where B_e is the rotational constant for the molecule at the equilibrium position, d_i is the degeneracy of the vibration ν_i ($d_1 = d_2 = d_3 = 1, d_4 = d_5 = 2$, for C_2H_2), and the a_i 's are constants small compared to B_e . Here it is also understood that $\nu = \nu_1 \nu_2 \nu_3 \nu_4 \nu_5$, the quantum number designation of the level. Thus, the energy of a Q-branch transition in emission between some upper level (U) and some lower level (L) is given, in the first approximation, by

$$Q(J) = [E_{\nu_U} - E_{\nu_L}] + B_L \ell^2_L - B_U \ell^2_U + (B_U - B_L)J(J+1) + \dots \quad (3-3)$$

or since the observed band center, ν'_0 , is given by⁽¹⁷⁾

$$\nu'_0 = \nu_0 - B_U \ell^2_U + B_L \ell^2_L \quad (3-4)$$

where ν_0 is the vibrational band center

$$\nu_0 = E_{\nu_U} - E_{\nu_L}$$

Thus, equation (3-3) can be written as

$$Q(J) = \nu'_0 + (B_U - B_L)J(J+1) + \dots \quad (3-4a)$$

This equation can be used to calculate the energies of the Q-branch lines of the $\nu_2 - \nu_5$ band of C_2H_2 . The results obtained using Herzberg's⁽¹⁶⁾ values of B_e and the a_i 's.

$$\begin{aligned}
 B_e &= 1.1838 \text{cm}^{-1} \\
 \nu'_0 &= 1245.28 \text{cm}^{-1}^* \\
 a_1 &= 0.008 \text{cm}^{-1} \\
 a_2 &= 0.0063 \text{cm}^{-1} \\
 a_3 &= 0.0056 \text{cm}^{-1} \\
 a_4 &= 0.0013 \text{cm}^{-1} \\
 a_5 &= 0.0022 \text{cm}^{-1}
 \end{aligned}$$

giving,

$$B_U = B_{\nu_2} = 1.17105 \text{cm}^{-1}$$

$$B_L = B_{\nu_5} = 1.17955 \text{cm}^{-1}$$

or,

$$\Delta B = B_U - B_L = 0.00850 \text{cm}^{-1}$$

are shown in Table 1 for the first 20 Q-branch transitions of the $\nu_2 - \nu_5^1$ band of C_2H_2 . Normally, for the C_2H_2 the lines with odd J should be more intense than the even J lines due to the 3:1 ratio of the statistical weights.⁽¹⁶⁾

The results obtained Keller's⁽¹⁷⁾ values of B_e , and the a_i 's,

$$\begin{aligned}
 B_e &= 1.1845 \text{cm}^{-1} \\
 \nu'_0 &= 1245.20 \text{cm}^{-1}^{**} \\
 a_1 &= 0.0063 \text{cm}^{-1} \\
 a_2 &= 0.0092 \text{cm}^{-1}
 \end{aligned}$$

*Herzberg gives a value for $\nu'_0 = 1244.7 \text{cm}^{-1}$. We have adjusted this value by 0.58cm^{-1} to give a better fit to the experimentally determined wavelengths.

**Keller's value for $\nu'_0 = 1244.79 \text{cm}^{-1}$. We have adjusted this value by 0.41cm^{-1} to give a better fit to the experimentally determined wavelengths.

Table 1. Q-Branch Lines of the $\nu_2 - \nu^1 5$ Band of C₂H₂ Calculated from Herzberg's Data

<u>J</u>	<u>ΔE</u>	<u>λ_{calc.}</u>	<u>λ_{obs.}</u>
1	1245.26	8.0282	
2	1245.23	8.0285	
3	1245.18	8.0288	
4	1245.11	8.0292	
5	1245.03	8.0298	
6	1244.92	8.0304	
7	1244.80	8.0312	8.0313*
8	1244.67	8.0321	
9	1244.52	8.0331	8.0329
10	1244.35	8.0342	
11	1244.16	8.0354	8.0352
12	1243.95	8.0367	
13	1243.73	8.0381	8.0383
14	1243.50	8.0397	
15	1243.24	8.0413	8.0416
16	1242.97	8.0431	
17	1242.68	8.0449	
18	1242.37	8.0469	
19	1242.05	8.0490	
20	1241.71	8.0512	

*This line observed only once.

$$a_3 = 0.0053 \text{ cm}^{-1}$$

$$a_4 = 0.0065 \text{ cm}^{-1}$$

$$a_5 = 0.0021 \text{ cm}^{-1}$$

giving,

$$B_U = 1.1673 \text{ cm}^{-1}$$

$$B_L = 1.1786 \text{ cm}^{-1}$$

or,

$$B = B_U - B_L = -0.0113 \text{ cm}^{-1}$$

are shown in Table 2 for the first twenty Q-branch transitions of the $\nu_2 - \nu_5^1$ band of C_2H_2 . All values of ΔE are given for vacuum and wavelengths are given in air.

A piezoelectric drive was used to scan one laser mirror to average mode pulling effects and assure mode coincidence with any rotational line having sufficient gain to lase. An indication of these effects is that while operating the drive we have seldom found that a rotational line is missing. This is commonly the case with a fixed cavity length. Thus, scanning the cavity provides the best (unshifted) lasing spectrum available.

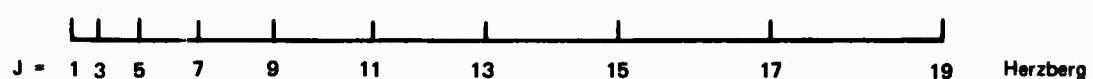
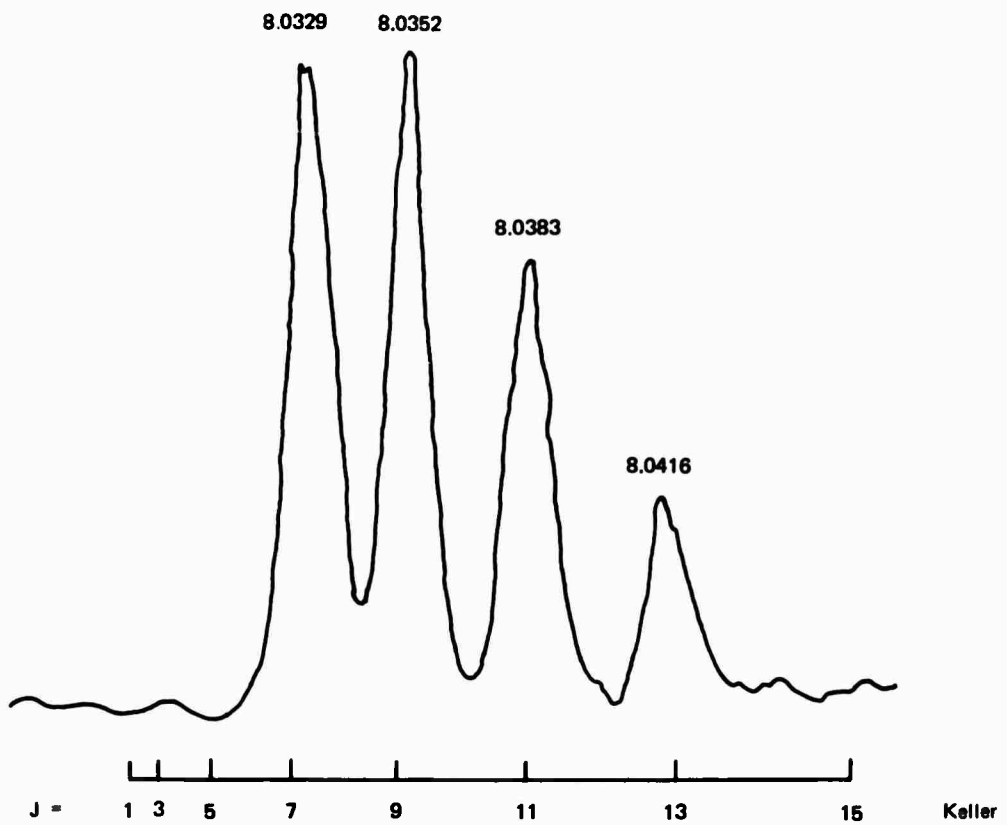
Phase sensitive synchronous amplification of a Ge:Au detector output was used; the amplifier gives a dc output proportional to the laser emission which is used as input to the Y-channel of an X-Y recorder. A potentiometer mounted to the wavelength drive of the spectrometer gave a dc voltage proportional to the wavelength which then drives the X-channel of the recorder. An additional moveable mirror and an S-1 PMT is used to enable the twelfth order of the Ne calibration lines to be recorded on the X-Y recorder along with the C_2H_2 laser lines. In all cases, dielectric mirrors were used. The total reflector has a five meter radius and a reflectivity of 99.5 percent ± 0.5 percent at 8 u. The output mirror is flat with a reflectivity of 98 percent ± 0.5 percent at 8 u.

Figure 10 shows a typical spectrum, and, in addition, shows the calculated wavelength of the rotational lines in the Q-branch for the rotational constants of Herzberg⁽¹⁶⁾ and Keller⁽¹⁷⁾. The best fit is seen using the rotational constants of Keller. Although this fit is quite reasonable, all doubts about the identification of the transition were removed by an absorption experiment.

Table 2. Q-Branch Lines of the $\nu_2 - \nu'_5$ Band of C_2H_2 Calculated from Keller's Data

<u>J</u>	<u>ΔE</u>	<u>$\lambda_{\text{calc.}}$</u>	<u>$\lambda_{\text{obs.}}$</u>
1	1245.18	8.0288	
2	1245.13	8.0291	
3	1245.06	8.0295	
4	1244.97	8.0301	
5	1244.86	8.0308	8.0313*
6	1244.73	8.0318	
7	1244.57	8.0327	8.0329
8	1244.39	8.0339	
9	1244.18	8.0352	8.0352
10	1243.96	8.0367	
11	1243.71	8.0383	8.0383
12	1243.44	8.0400	
13	1243.14	8.0419	8.0416
14	1243.82	8.0440	
15	1242.49	8.0462	
16	1242.13	8.0485	
17	1241.74	8.0510	
18	1241.34	8.0536	
19	1240.91	8.0564	
20	1240.45	8.0594	

*This line only observed once.



The lines at the bottom indicate the wavelengths of the rotational lines as calculated from the constants of Keller and Herzberg as discussed in the text.

AJ0800-1

Figure 10. The Output Spectra of the Acetylene Laser

The absorption apparatus is indicated in Figure 11 and includes an additional gas cell inside the laser resonator. The plasma tube and the absorption cell are separated by a Brewster angle NaCl window. Only two rotational lines (Q(7) and Q(9)) were observed with this configuration even when a piezoelectric drive was used to scan one of the laser mirrors.

The laser spectra for three different C_2H_2 pressures in the absorption cell are shown in Figure 12. A pressure of 1.5 Torr was sufficient to prevent laser emission. However, laser emission was unaltered when the cell was opened to air at one atmosphere. Therefore, we conclude that molecular acetylene is definitely the lasing specie.

In an additional experiment, the absorption cell was placed outside the laser resonator, and the absorption was measured as a function of pressure and temperature. This data is shown in Figure 13. The measurements at the lower temperature were made with dry ice packed around the stainless steel absorption cell. A theoretical fit was made with the following expressions and is indicated by the solid curves:

$$D_J = \frac{C_1 P B_L e^{-729/kT} (2J+1) e^{-B_L J(J+1)/kT}}{T(T^{1/2} + C_2 T^{-1/2} P)(1 + e^{-619/kT} + e^{-729/kT})} \quad (3-5)$$

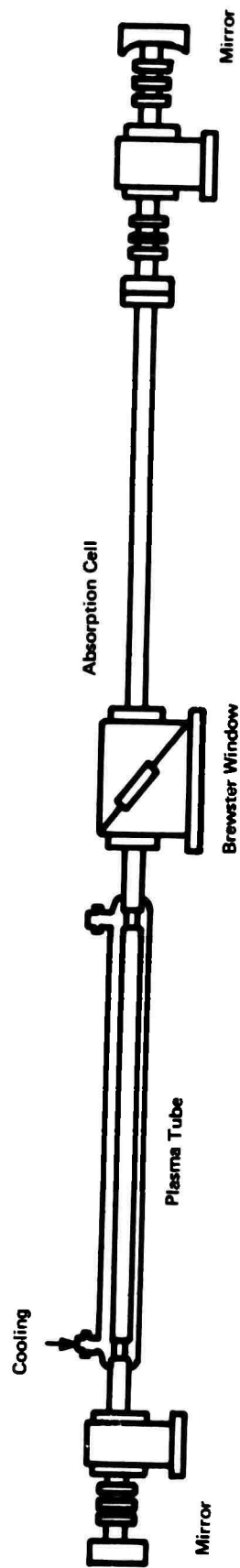
$$D = -\log_e \frac{\sum W_J D_J}{\sum W_J} \quad (3-6)$$

where $J = 7, 9, 11$, and 13 ; and W_J is a weighting factor to take the different intensities of the rotational lines into account.

$$C_1 = \frac{\lambda^3 A_{21}}{8\pi} \sqrt{\frac{M}{2\pi k^3}} \quad (3-7)$$

and

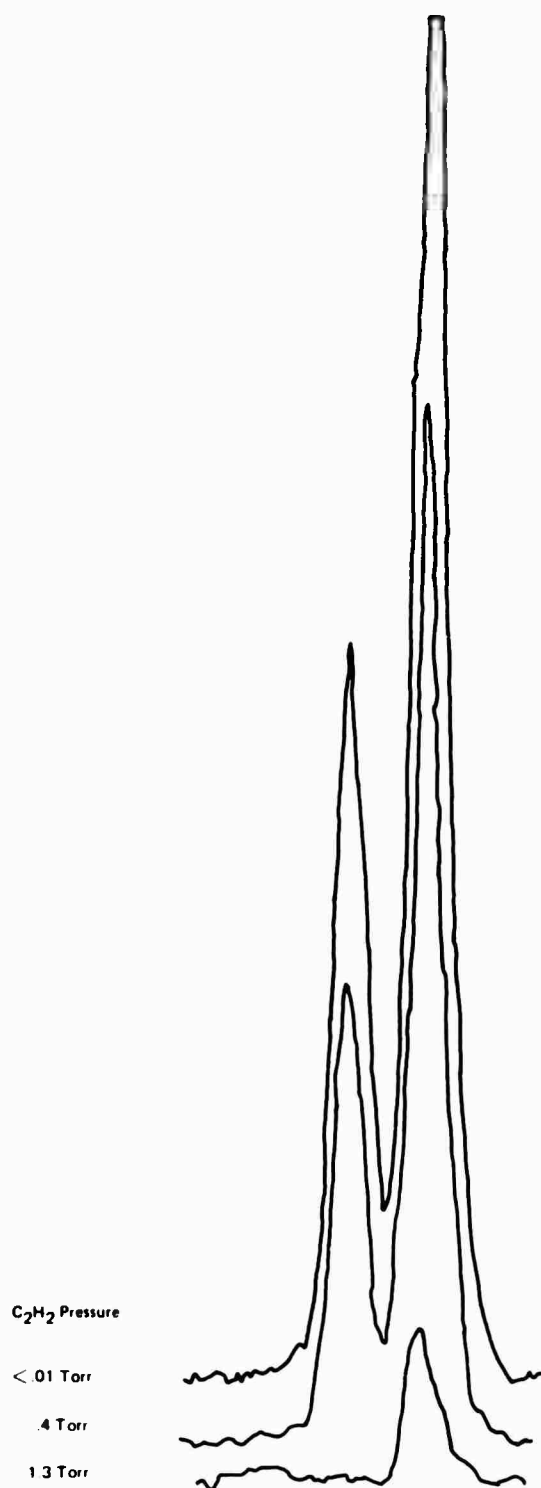
$$C_2 = \frac{\sigma}{\pi \lambda k} \sqrt{\frac{2}{\pi \log_e 2}} \quad (3-8)$$



The plasma tube and the absorption cell are separated
by a NaCl window oriented at Brewster's angle.

AK0800-1

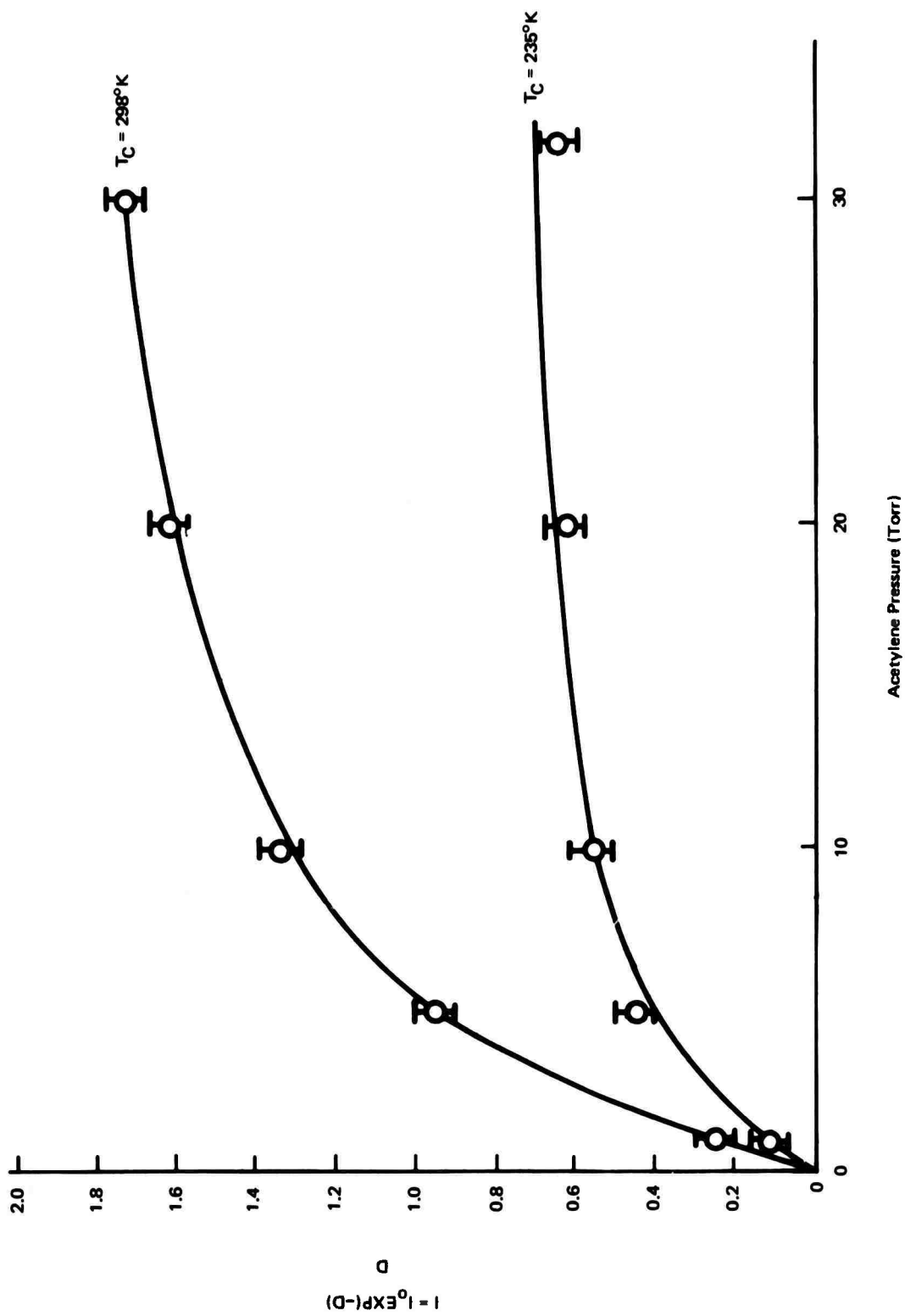
Figure 11. Intracavity Absorption Apparatus



Laser output spectra observed in the intracavity absorption experiment. Only two rotational lines were above threshold with the cell in place. As acetylene, at room temperature, was added to the cell, the laser output was quenched.

AL0800-1

Figure 12. Intracavity Absorption Experiment



The solid curves were calculated from the expression in Eq. 3-5 as discussed in the text.

Figure 13. Acetylene Pressure (Torr)

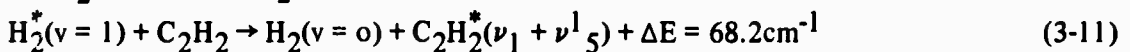
T is the temperature in K° , P is the pressure in Torr, k is Boltzmann's constant = $0.6951 \text{ cm}^{-1} \text{ K}^{-1}$, B_L is the rotational constant = 1.1786 cm^{-1} , M is the molecular mass, and A_{21} is Einstein's "A" coefficient for the transition. σ is a collisional cross-section. The constants $C_1 = 5300$ and $C_2 = 51.79$ were established by fitting the data at room temperature. In order to fit the low temperature results, a temperature = $235^\circ K$ was required. This is $40^\circ K$ higher than the temperature of dry ice, but no measurement of temperature was made inside the cell, and small portions were not cooled at both ends. Thus, the accuracy of this temperature is not known.

The absorption data given above is sufficient to establish that a lower lasing state is in the ν_5^1 band.

The absorption measurements also provide an estimate of the laser gain. Based on an active length of 85cm and a total inactive length of 60cm in the plasma tube, and an acetylene pressure of 1.5 Torr in the intracavity absorption cell, one calculates a peak gain of 2.9db/meter.

3.3 DISCUSSION OF POSSIBLE PUMPING MECHANISMS

Since the laser emission is occurring on Q-branch transitions of the $C_2H_2 \nu_2 - \nu_5^1$ band, the laser could then be functioning as a classical four level laser (refer again to Figure 9). Two possible pumping mechanisms for obtaining population inversion in C_2H_2 are direct electron impact excitation and a near resonant vibrational energy transfer from the $H_2^*(v=1)$ which has been excited by electron impact in the helium rich plasma.



The excited state produced by the inelastic collision process shown in Equation (3-9) is not indicated since the details of this process are not known, nor is the relative importance of this mechanism known. The $C_2H_2^*(\nu_1 + \nu_5^1)$ level on the right side of process (3-11) can cascade via collisions or radiative transitions to the ν_2 level, which is the upper laser level. The lower laser level, the ν_5^1 level, can be de-populated through the strongly allowed ν_5^1 to the ground vibration level transition.

Vibrationally excited, ground-electronic-state hydrogen molecules have been observed as a long-lived product of a microwave discharge in pure hydrogen gas by Heidner and Kasper.⁽¹⁸⁾ These excited molecules were identified by their vacuum-ultraviolet absorption spectrum. They concluded that, at a pressure of three torr, hydrogen passed through a microwave discharge contains approximately one to four percent of the molecules in the $v'' = 1$ state 25 msec after leaving the discharge. This compares with 30 percent of the N_2 molecules in the $v'' = 1$ state in a low pressure microwave discharge in pure N_2 as determined by Kaufman and Kelso.⁽¹⁹⁾

The relaxation time of the $H_2^*(v = 1)$ level should be about 250 msec at $T = 300^\circ K$ and $p = 3$ torr.^(18,20) This compares to the relaxation time of 114 msec of $N_2^*(v = 1)$ at $T = 300^\circ K$ and pressures of the order of a few torr as determined by Morgan and Schiff.⁽¹⁴⁾

The cross section as a function of electron energy, $\sigma(E)$ for the process (3-6) has been measured by Schulz.⁽²¹⁾ It has a peak value of $0.55 \times 10^{-16} \text{ cm}^2$ at 2.2 ev compared to a peak value of $1.5 \times 10^{-16} \text{ cm}^2$ at 2.2 ev for the vibrational excitation of N_2 by direct electron impact. From $\sigma(E)$, the rate coefficient for the excitation of H_2 by direct electron impact can be calculated.⁽²²⁾

$$X(t) = N_e(t) \langle \sigma v \rangle \quad (3-12)$$

where $N_e(t)$ is the electron density in the plasma and $\langle \sigma v \rangle$ is Schulz's cross section averaged over the electron velocity distribution in the plasma. Assuming a Maxwellian energy distribution for the electron in the plasma,

$$\langle \sigma v \rangle = K_0 T_e^{-3/2} \int E \sigma(E) e^{-E/T_e} dE \quad (3-13)$$

where $K_0 = 6.6971 \times 10^7$ and T_e is the average electron temperature in ev. The term $\langle \sigma v \rangle$ given by Equation (3-9) is plotted versus electron temperature in Figure 14. It is clear from Equations (3-8), (3-9), and from Figure 14 that the rate coefficient for vibrational excitation of H_2 by direct electron impact depends upon the electron temperature and the electron density in the plasma.

Data is available in the literature on the electron temperature in pure gases under normal glow discharge conditions, but very little data is available for gas mixtures. The electron temperature, T_e , as a function of ionization potential, u_i , pressure, p , and tube radius, R , and an empirical constant, c , which depends on the gas, is given by Brown⁽¹³⁾ (see also von Engel,⁽²³⁾ pages 63 and 242).

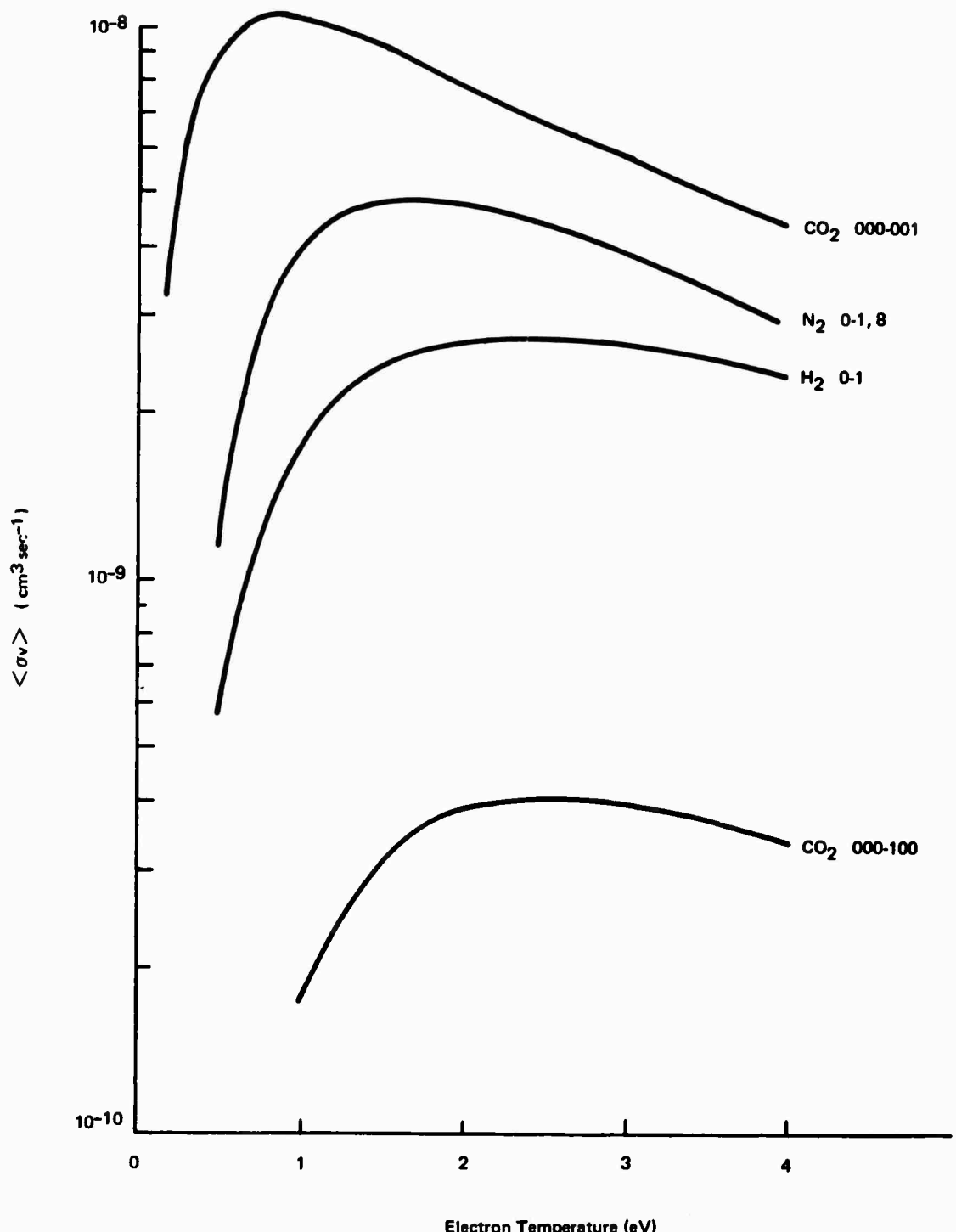


Figure 14. $\langle \sigma v \rangle$ vs. Electron Temperature

AN0800-1

$$\left(\frac{U_i}{T_e}\right)^{1/2} \exp\left(\frac{U_i}{T_e}\right) = 1.16 \times 10^7 c^2 p^2 R^2 \quad (3-14)$$

The derivation of this equation is also presented in Reference 1. The electron temperature versus pressure in the positive column of a low pressure gas discharge in pure N₂, pure N₂, pure H₂ and pure He calculated from Equation (3-10) is shown in Figure 15. This equation only considers the ionization potential of the gas in determining the electron energy.

The source of electrons in a glow discharge is from ionization of the component gases and from secondary emission from the cathode. The energy of the electrons is controlled by elastic and inelastic collisions with the component gases. The inelastic processes are ionization and electronic excitations of all the components of the plasma, and vibrational and rotational excitations of the molecular components.

Considering only the effect of the ionization potential, it can be shown that the electron temperature in a mixture of H₂-He can be somewhat higher than for H₂ alone at the same total pressure.⁽¹⁾ This same argument can be applied to H₂-C₂H₂-He and C₂H₂-He mixtures. This implies that high He partial pressures can be used to stabilize the discharge and still maintain high electron temperatures.

The use of pulsed excitation for H₂-C₂H₂-He also increases the excitation rate through the higher current density obtainable, by at least an order of magnitude, compared to dc operation with the gas mixtures used.

Laser action in H₂-C₂H₂-He could only be obtained over a very narrow range of acetylene pressures. Laser emission was not observed from a pure C₂H₂ plasma or a C₂H₂-H₂ plasma, but it was observed with a C₂H₂-He plasma. Figure 16 shows the results when the hydrogen was removed from the discharge. In the upper curve, the pressures of H₂-C₂H₂-He were 2, 1, and 32 torr, respectively, and in the lower curve the pressures were 0, 1, 32 torr. In both cases, both the gas and cooling jacket were at -60°C. Without hydrogen, the peak power was reduced by a factor of two, and the pulse energy was reduced even more because of the slight decrease in pulse width. The same spectral lines were observed in the laser output with or without hydrogen.

Further experiments were carried out to characterize the behavior of the laser in the absence and presence of H₂. Data was taken in a new one inch I.D. plasma tube with coaxial

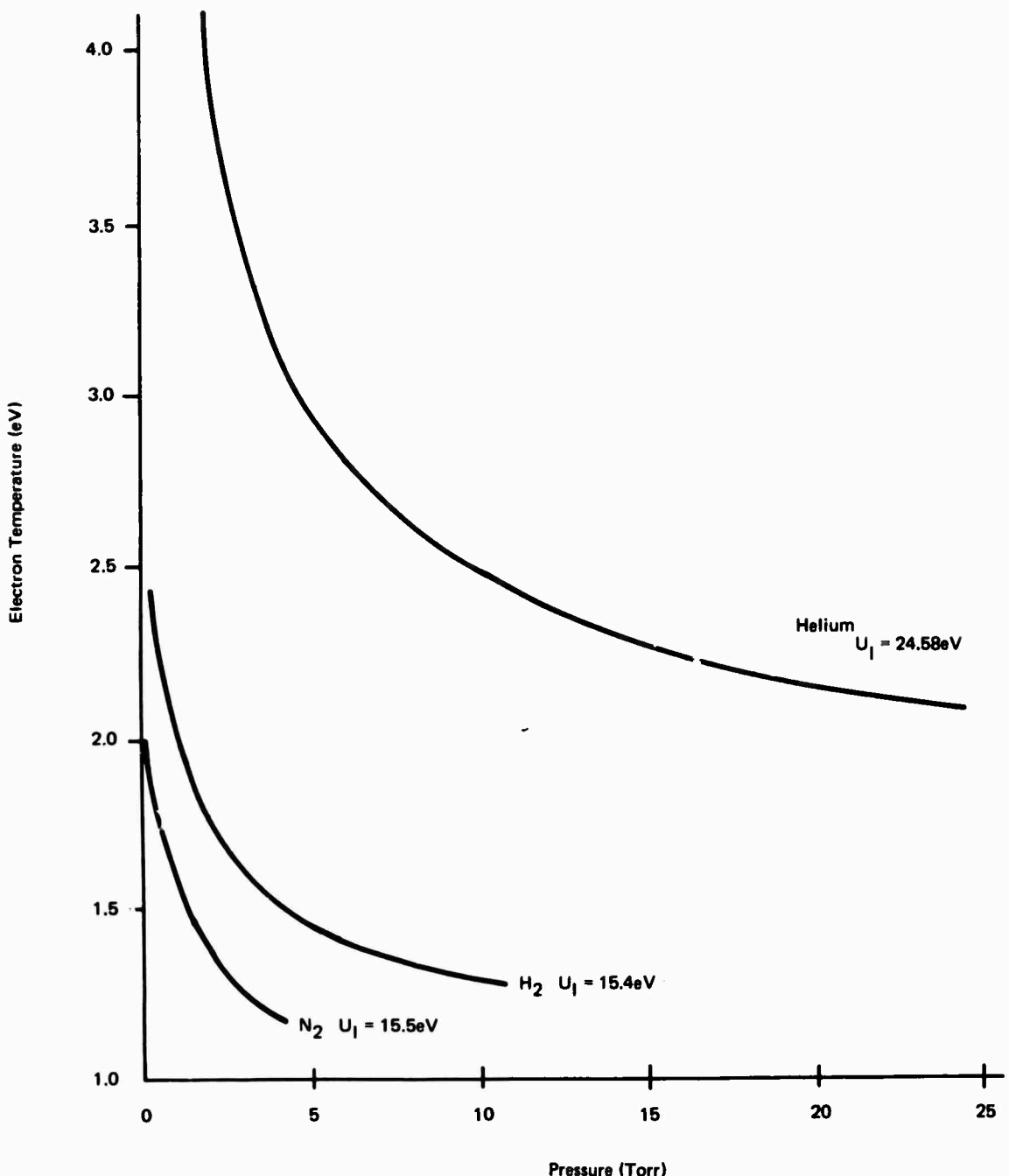


Figure 15. Electron Temperature vs. Pressure in Pure Gases

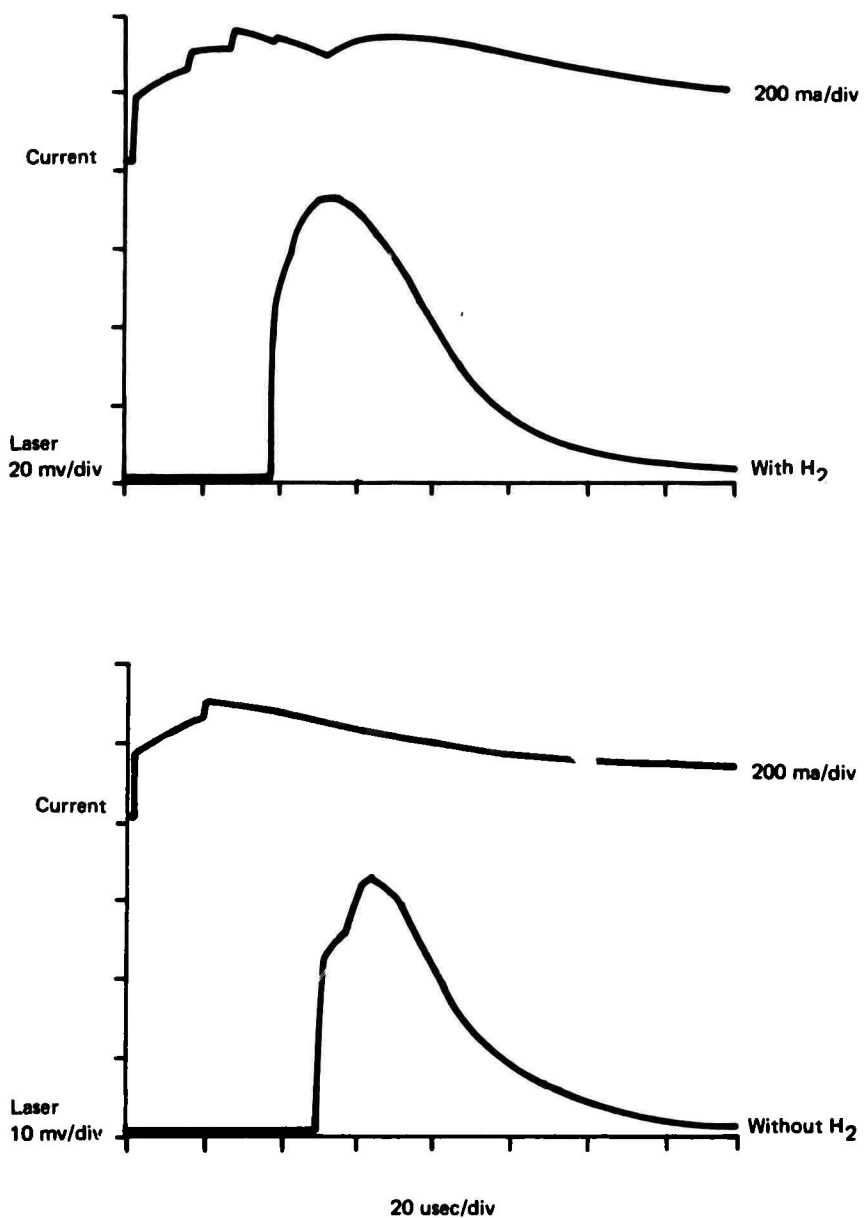


Figure 16. Operation of the acetylene laser without hydrogen

electrodes, and the results are given in Table 3. The flow rates for the $C_2 H_2, H_2, N_2$ and He are given in terms of the centimeters of deflection on the flow meters, and the average power at 26Hz was measured with an Eppley thermopile. In all cases, the laser operated better with H_2 present in the discharge tube although the degree of improvement depends upon the acetylene flow. This is shown in Figure 17. Thus, at higher acetylene flow rates the hydrogen is much more critical.

The substitution of N_2 for H_2 is detrimental to the operation of the laser. With acetylene flow rates corresponding to 0.9 and 1.5cm the addition of N_2 caused the laser to cease operation.

The visible emission from the plasma tube was examined for identical discharge conditions to those indicated in Table 1. Light was collected through a NaCl window on the cathode end of the plasma tube and monitored with a one meter spectrometer and a photomultiplier tube. Some of the results are shown below. Figure 18 is the spectra of the CH or methyne radical at 4314Å with the flow rates corresponding to cases 1 and 2 Table 1. The intensity of the CH band is reduced by the addition of H_2 . Similar results were obtained for the C_2 Swan band at 5165Å shown in Figure 19. Thus, the addition of H_2 to the C_2H_2/He discharge decreases the number of dissociative products from the acetylene. This also corresponds to the case of maximum laser output, and is consistent with the conclusion that acetylene and not a discharge product is the lasing species.

Figure 20 gives the spectra of the CH band for the substitution of N_2 for H_2 and corresponds to cases 2 and 3 in Table 1. The intensity of the band is once again reduced. Note the appearance of the N_2^+ band at 4278Å when N_2 is added.

There are several possible explanations for the observed behavior. First, since the laser operates without H_2 , direct impact excitation is obviously effective in populating the upper laser state. However, it is conceivable that this pumping mechanism is saturable, and resonant energy transfer from vibrationally excited hydrogen becomes more important at the higher acetylene pressures. This does not explain, however, the measurements of the intensities of the CH and C_2 bands.

A second possible explanation is that the addition of H_2 lowers the electron "temperature" in the discharge resulting in fewer acetylene molecules being dissociated and, in addition, creates more optimum conditions for generating a population inversion in the gas.

Table 3. Effects of H₂ and N₂ on the C₂H₂ Laser

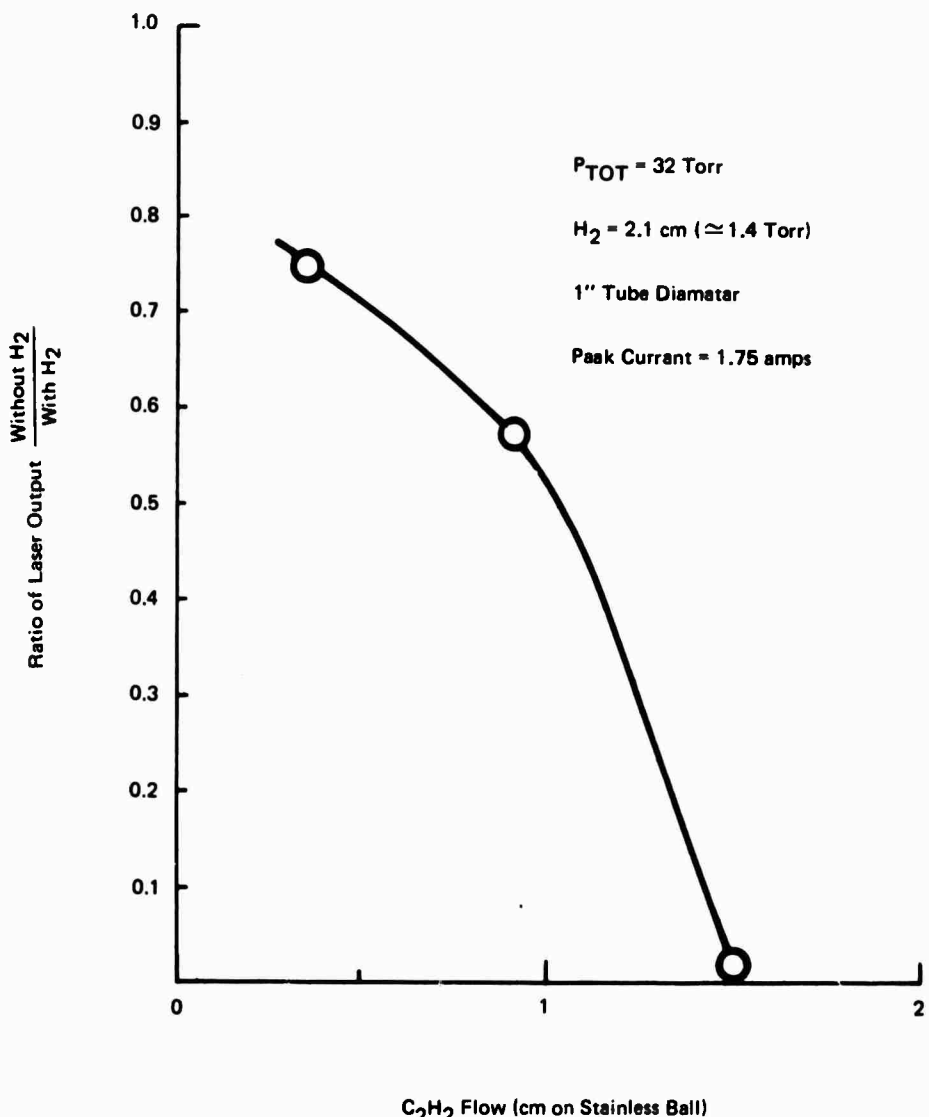
	<u>C₂H₂</u>	<u>H₂</u>	<u>N₂</u>	<u>He</u>	<u>T</u>	<u>Ave. Pwr.</u>
1.	0.35	2.1	0	25+	-17°C	14 mW
2.	0.35	0	0	25+	-18	10.5
3.	0.35	0	2.1	25+	-17	2.1
4.	0.9	2.1	0	25+	-16	19.6
5.	0.9	0	0	25+	-17	11.2
6.	0.9	0	2.1	25+	-17	-
7.	1.5	2.1	0	25+	-16	14
8.	1.5	0	0	25+	-16	0.28
9.	1.5	0	2.1	25+	-17	-

Total pressure in all cases was 32 Torr

Peak current was 1.75 amp

26 Hz rep. -rate

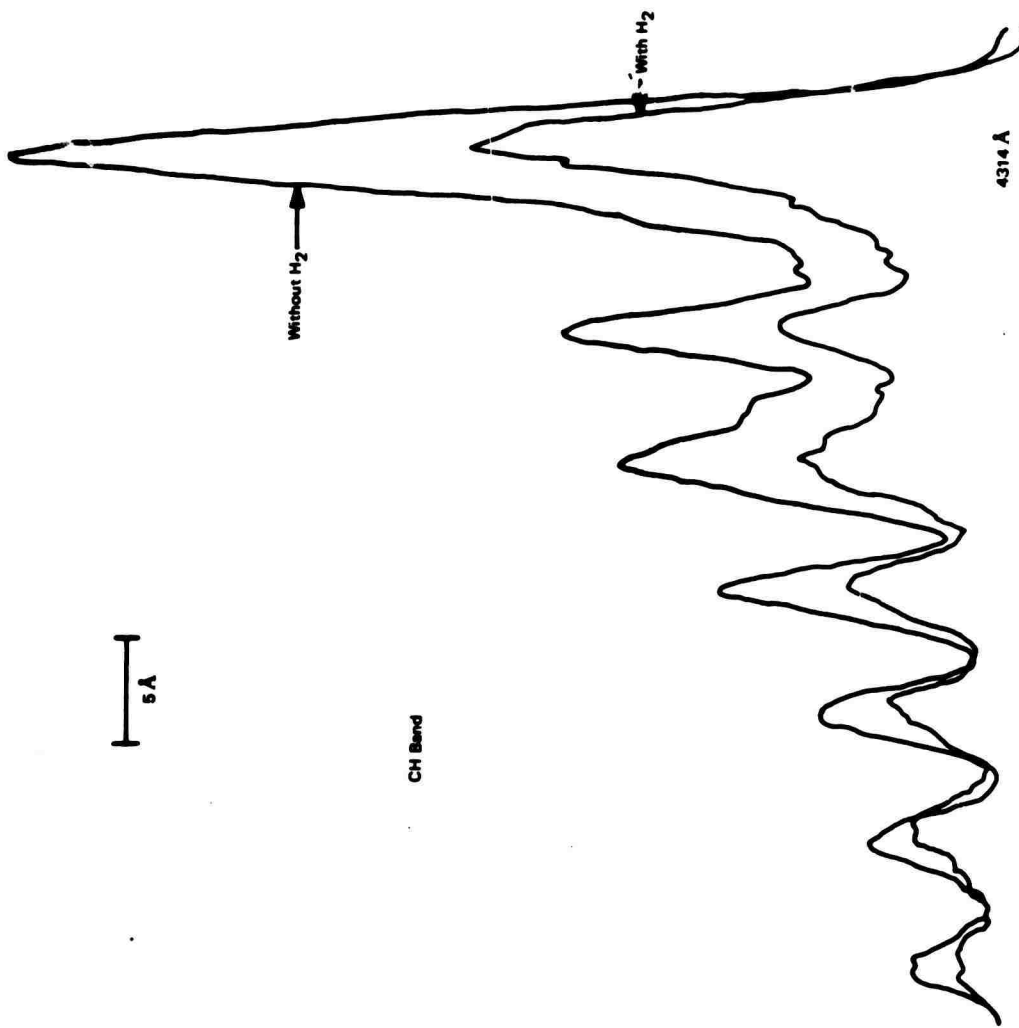
C ₂ H ₂ - 0.35 cm	0.4 Torr
H ₂ - 2.1	1.3 Torr
He - 25+	30.3 Torr



The ratio of laser output with and without hydrogen is plotted as a function of acetylene partial pressure. The laser output is highly dependent on the presence of hydrogen at the higher acetylene pressures. Total pressure in the discharge was kept constant by replacing hydrogen by helium when the data was recorded.

AQ0800-1

Figure 17. Effect of Hydrogen on the Acetylene Laser Output



The total pressure in the discharge was kept constant by replacing the hydrogen with helium.

Figure 18. Intensity of a CH Band With and Without Hydrogen

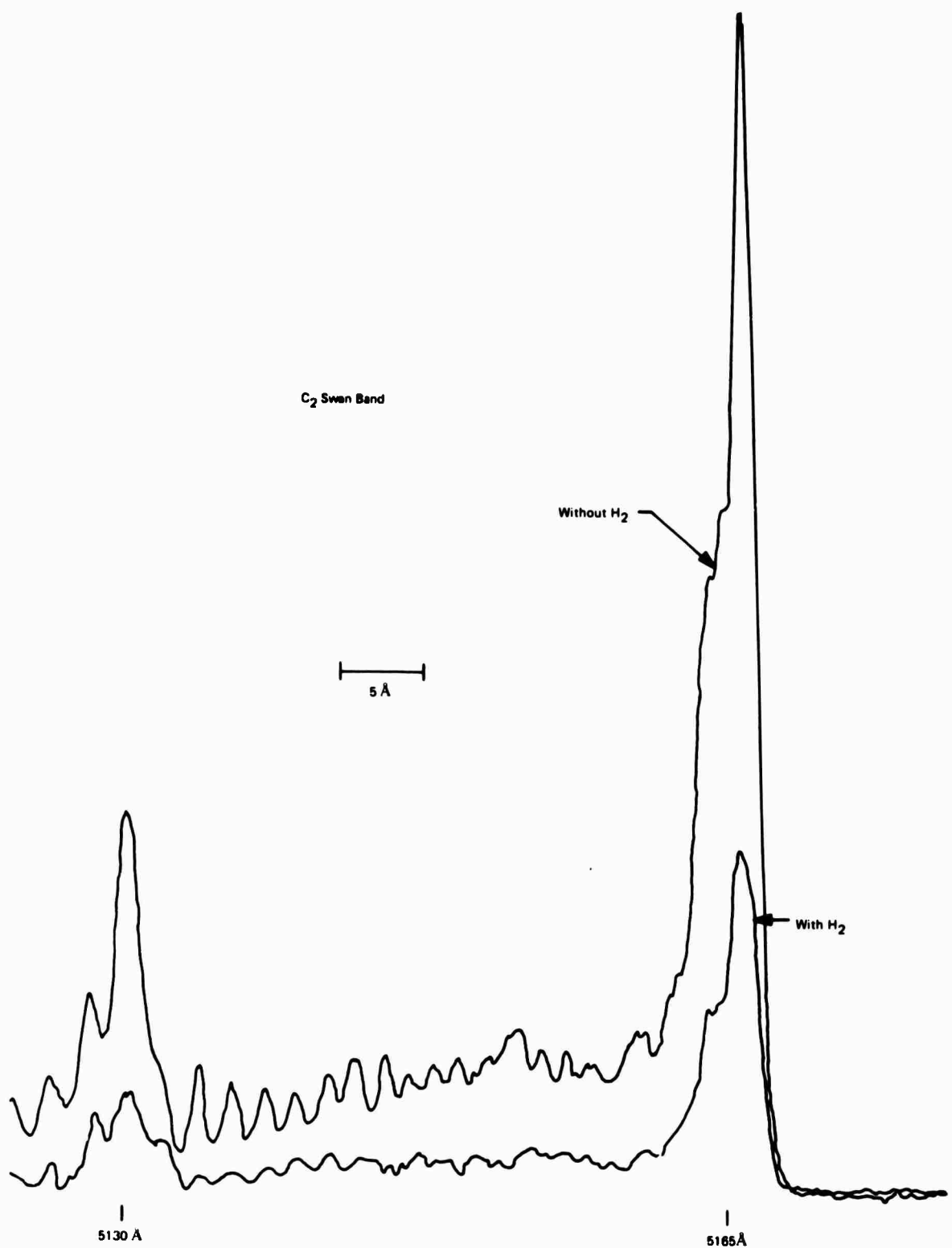
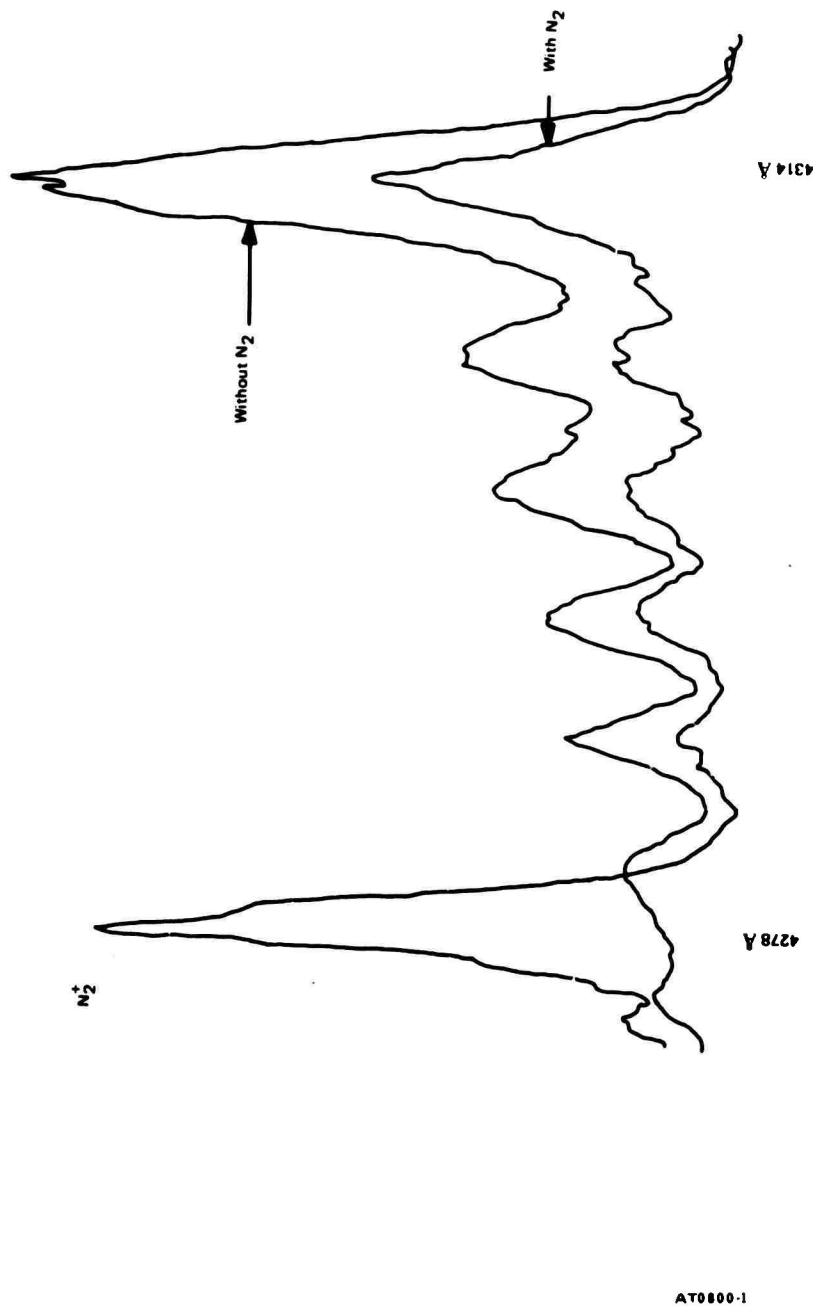


Figure 19. Intensity of a C₂ Swan Band With and Without Hydrogen

CH Band



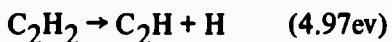
In this experiment nitrogen was substituted for hydrogen in the mixture. Then the CH band was monitored as nitrogen was removed. Note the line in the first negative system of N_2^+ which appears in the presence of nitrogen at 4278 Å.

Figure 20. Intensity of a CH Band With and Without Nitrogen

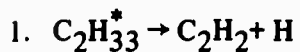
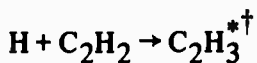
Finally, the possibility exists that the hydrogen prevents the dissociation of acetylene, thus keeping the active species in the lasing volume for greater periods of time. The energy required to break the triple bond between the carbon atoms is 9.95ev, but once this bond is broken, it is virtually impossible to reform it and these molecules are permanently lost from the lasing process.



In addition, a hydrogen atom can be removed with an energy of 4.97ev leaving the highly reactive C_2H radical.

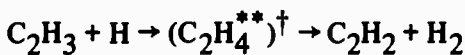
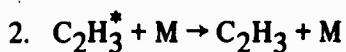


With excess H_2 present in the plasma tube, however, additional atomic hydrogen is produced (dissociation energy = 4.47ev) and can lead simply to a recombination of atoms without consumption of acetylene. At least two possible reactions exist and start with the hydrogenation of acetylene:⁽²⁴⁾



Thus, acetylene is reformed in the discharge rather than being split into dissociative products.

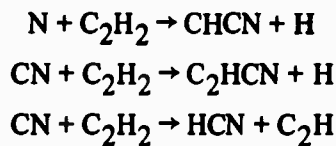
The excited C_2H_3^* can also collide with a third molecule reducing the excess energy and then interact with atomic hydrogen to reproduce acetylene and molecular hydrogen.



[†] $(\text{C}_2\text{H}_4^{**})$ is formed with 63 kcal/mole excess energy above its dissociation energy to form $\text{C}_2\text{H}_2 + \text{H}_2$.⁽²⁴⁾

[†]The * indicates that this molecule is vibrationally excited beyond the dissociation limit. Species without the * may still possess vibrational energy but below the dissociation limit.

On the other hand, replacement of hydrogen by nitrogen can lead to the consumption of acetylene by several reactions.⁽²⁵⁾ The mechanisms given below are typical.



Such destruction of acetylene is consistent with the observation that the substitution of nitrogen for hydrogen is detrimental to the laser performance.

We conducted experiments with the parallel tube shown in Figure 4 to test the hypothesis of vibrational energy transfer from excited hydrogen to acetylene. A pulsed discharge in mixtures of hydrogen and helium occurred in the side-arm or discharge region of the tube. The gases then flowed into the interaction region of the tube where they were mixed with acetylene at room temperature. In each experiment, the mirrors were aligned by filling the tube with $\text{N}_2\text{-CO}_2\text{-He}$ and adjusting for maximum average power.

A wide range of gas mixtures, flow rates, and total pressures were tried, and estimates indicate that hydrogen flow velocities up to 20 meters per second were present. In all cases, the results were negative, and we have not observed laser emission from C_2H_2 in the parallel discharge tube.

Two problems with this experiment immediately come to mind: 1) the lower level population in acetylene, and 2) vibrational deactivation by collisions with the wall. The lower level of the lasing transition is only 729cm^{-1} above the ground state of acetylene. Thus, at room temperature, the population of the lower laser level is 3 percent to 4 percent of the ground state population. Larger inversions are required than for the case of CO_2 , and the unpumped parts of the interaction region may be a sufficiently large fraction of the total length so that the gain cannot exceed the losses.

Diffusion coefficients have been used to estimate the lifetime of vibrationally excited H_2 if wall collisions are the source of deactivation. The mutual diffusion coefficient, D_{12} , for a binary mixture of hard, elastic spheres is⁽²⁶⁾

$$D_{12} = \frac{3}{8} \left[\frac{\pi k T}{2M_r} \right]^{1/2} \frac{1}{\pi N d_{12}}$$

where M_r is the reduced mass $\frac{M_1 M_2}{M_1 + M_2}$

$N = N_1 + N_2$ is the total number of molecules, and

$d_{12} = \frac{d_1 + d_2}{2}$ is the average molecular diameter.

If each collision results in a deactivation, the average lifetime of an excited specie in an infinite cylinder of radius, r_0 , is

$$\tau = \frac{1}{D_{12}} \left\{ \frac{\tau_0}{2.405} \right\}^2$$

Table 4 shows the results of lifetime calculations using these equations. The first entry is representative of the conditions in the parallel tube which results in lifetime of 0.732 msec. Thus, even at the highest estimated flow velocity for hydrogen (2.0 cm/msec), the excited molecules would only travel several centimeters before a very large fraction were deactivated. In our tube, the molecules have to travel approximately 10 cm to reach the interaction region, so if wall collisions are effective it is unlikely that significant numbers of vibrationally excited hydrogen are available to pump the acetylene.

The second and third entries in the table represent the conditions in the simpler, pulsed tube, and the calculations show lifetimes three to four times greater than those expected in the parallel tube. The last entry is representative of the situation of N_2 - CO_2 -He in the parallel tube. Based strictly on this lifetime of 2.2 msec, one would come to the same conclusions reached above and predict that CO_2 would not work in the parallel tube. This is obviously an erroneous conclusion as evidenced by the pulsed and CW operation reported in Section 2. Thus, some of the assumptions used in the calculation may be incorrect, at least for the N_2 -He case. The Lewis-Rayleigh after-glow, which is a good indication of excited molecular nitrogen, can be seen throughout the interaction region and even some distance from the laser in the glass tubing leading to the vacuum pumps. In addition, the effectiveness of deactivating collisions with He has not been ascertained, and the small molecular weight of H_2 in contrast of N_2 may have important implications to the pumping process.

In summary, we have not demonstrated that energy transfer from vibrationally excited molecular hydrogen is instrumental in establishing the population inversion for the

Table 4. Lifetime by Diffusion to Walls

Pressures (Torr)			Temp (°K)	D_{12} (cm ² /sec)	τ (msec.)
H ₂	He	N ₂			
5	5		300	95.2	0.732
2	28		300	31.7	2.196
2	28		193	25.5	2.738
	5	5	300	40.6	1.719

$$d_{H_2} = 2.74 \text{ \AA}$$

$$M_{H_2} = 2.016$$

$$r_0 = 0.635 \text{ cm}$$

$$d_{He} = 2.18 \text{ \AA}$$

$$M_{He} = 4.002$$

$$d_{N_2} = 3.75 \text{ \AA}$$

$$M_{N_2} = 28.2$$

$\text{H}_2\text{-C}_2\text{H}_2\text{-He}$ laser. Direct electron excitation is important, however, and we have observed a correlation between the intensity of light from the visible emission bands of several dissociation products in the discharge and the operation of the laser. It is quite possible that the presence of hydrogen modifies the rates of dissociation through the mechanisms discussed above and improves laser operation by sustaining the number of C_2H_2 molecules in the discharge.

3.4 ATTEMPTS TO OBTAIN THREE TO FIVE MICRON EMISSION

There are a number of transitions between three to five microns in C_2H_2 . The bands observed by Keller are shown in Table 5. It is unlikely that the fundamental, combination, and overtone bands terminating on the ground state could produce laser emission because of the difficulty in obtaining sufficient population inversion. Thus, our interest centered on those bands involving the low-lying ν_4^1 and ν_5^1 levels.

The most likely transitions for laser action are probably in the $\nu_1 - \nu_5^1$ and $\nu_3 - \nu_4^1$ bands. However, the ν_4^1 level is not radiatively coupled to the ground state because of symmetry and one might expect a bottleneck to develop at the lower lasing state.

Since both of the potential laser transitions terminate on levels relatively close to the ground state, it is necessary to eliminate as much unexcited gas from the optical path as possible. Therefore, the plasma tube shown in Figure 21 was constructed. The windows were made of BaF for ease in alignment and were placed as close to the positive column as was mechanically feasible.

This new plasma tube was tested with CO_2 . The ratio of $\text{N}_2:\text{CO}_2:\text{He}$ was 2:1:4, and with an output mirror reflectivity of 95 percent and a total pressure of 10 Torr, the laser produced an output pulse energy of 17 millijoules. This pulse energy is quite comparable to that obtained from the simple tube with internal mirrors described in Section 2. With a 65 percent reflective output mirror, the laser produced 33 millijoule pulses.

Next, the plasma tube was tested with $\text{H}_2\text{-C}_2\text{H}_2\text{-He}$ and eight micron mirrors, and power measurements were made with an Eppley thermopile. The operation of the acetylene laser at eight microns was, in general, inferior to the operation in both the 1/2" and 1" I.D. tubes with internal mirrors. The improvement in performance expected due to the elimination of unexcited gas in the optical path was not observed.

Table 5. Some Infrared Transitions in Acetylene

<u>Band</u>	<u>Band</u>
	<u>Center (cm⁻¹)</u>
$4\nu_5^0 - \nu_5^1$	2151.4
$4\nu_5^2 - \nu_5^1$	2160.2
$3\nu_5^1$	2169.1
$\nu_1 - \nu_5^1$	2643.4
$\nu_3 - \nu_4^1$	2670.0
$\nu_2 + \nu_4^1 + \nu_5^1 - \nu_4^1$	2682.9
$\nu_2 + 2\nu_5^0 - \nu_5^1$	2691.0
$\nu_2 + \nu_5^1$	2701.6
ν_3	3281.5
$\nu_2 + \nu_4^1 + \nu_5^1$	3294.6

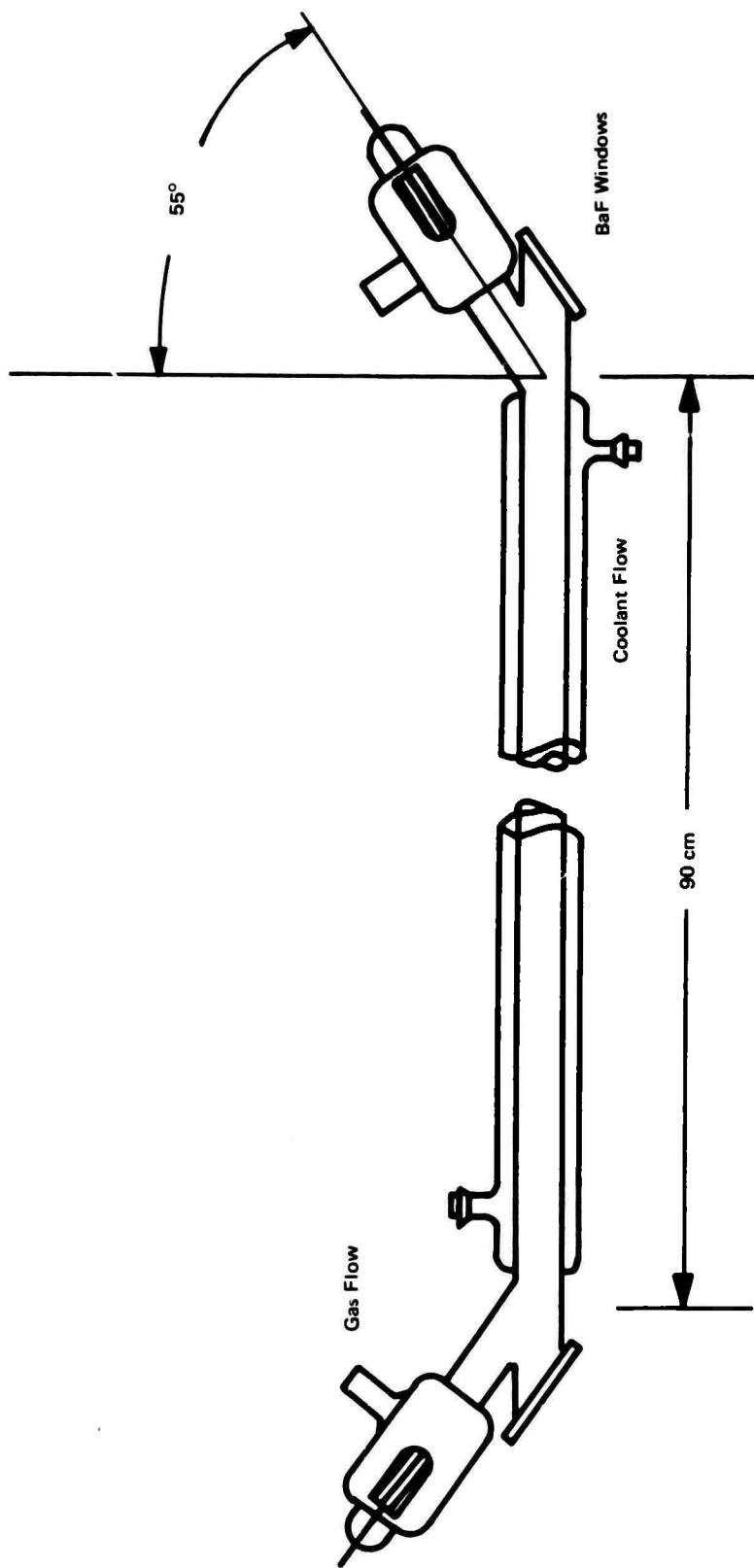


Figure 21. Plasma Tube Designed to Reduce Unexcited Gas

AU0800-1

Initial alignment at four microns was accomplished with a He-Ne laser. There was enough reflectivity from the four micron dielectric mirrors at 10.6 microns to operate a CO₂ laser, and the alignment was refined by filling the plasma tube with N₂-CO₂-He and adjusting the mirrors for maximum average power[†].

A wide range of H₂-C₂H₂-He gas mixtures and flow rates were tried unsuccessfully at temperatures as low as -40°C. Total pressures for the mixtures were varied from a few Torr to magnitudes which prevented discharge at voltages up to 14,000 volts. Finally, the energy storage capacitors were changed to provide different discharge conditions, again with no success.

[†]The mirror reflectivities at 4 microns were 99.4 percent and 98 percent, respectively.

Section 4. OTHER GASES

The results obtained with acetylene created little hope of finding laser emission in other gases between three to five microns. The crucial resonant energy transfer from H_2^* had not been verified, and, in fact, the eight micron laser worked rather well (at low acetylene pressures) with no H_2 at all. In addition, attempts to achieve four micron laser emission in acetylene had failed.

However, the preceding experiments had been limited in time and scope, and interpretation of the results could not be conclusive. Therefore, it was decided to spend the final weeks of the contract investigating a few additional gases.

A number of polyatomic molecules, such as NH_3 , CH_4 , and H_2O , have vibrational energy levels which are near resonance with the $v=1$ level of H_2 at 4159.2 cm^{-1} . Brief sketches of the energy levels in these molecules are given in the following paragraphs.

Ammonia- NH_3 . Ammonia is a symmetrical, pyrimidal molecule with four normal modes. The vibrational levels of NH_3 are shown in Figure 22. Some of the possible transitions resulting from vibrational energy transfer from H_2 are shown there and listed in Table 6. The 0102, 1100 and 0110 levels are all situated near the $4159.2\text{ cm}^{-1} H_2^* (v=1)$ level with the 4176 cm^{-1} 0102 level having the nearest resonance. The two energy levels shown for each of these vibrational modes come about because the v_2 mode is split by inversion doubling where the N atom is moved through the H_3 plane to an equivalent position on the other side.

Methane- CH_4 . The polyatomic molecule CH_4 has four normal modes of vibration, v_1 , v_2 , v_3 and v_4 . The 0011, 0102, 1001 and 0110 levels are all situated near the $H_2^* (v=1)$ energy level as shown in Figure 6. The transitions which might result from selectively populating one of these levels are shown in Figure 23 and are listed in Table 7.

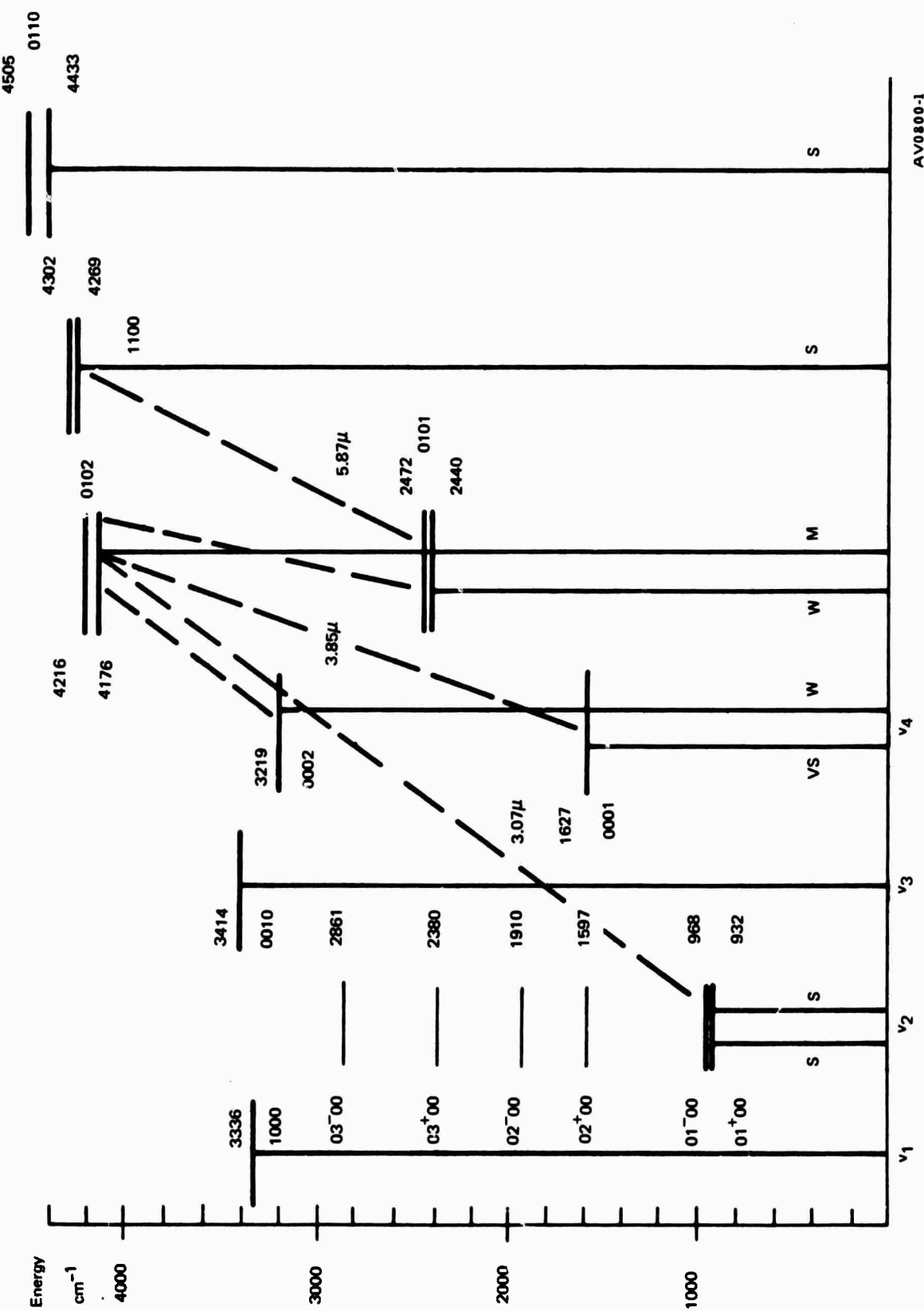


Figure 22. Vibrational Energy Level Diagram of Ammonia

Table 6. Possible Vibrational Transitions in Ammonia - NH₃

<u>VIBRATIONAL TRANSITION</u>	<u>ENERGY</u>	<u>WAVELENGTH</u>
0102 → 0100	3248 cm ⁻¹	3.07 μ
0102 → 0001	2589 cm ⁻¹	3.85 μ
0102 → 0002	997 cm ⁻¹	10.00 μ
0102 → 0101	1704 cm ⁻¹	5.87 μ

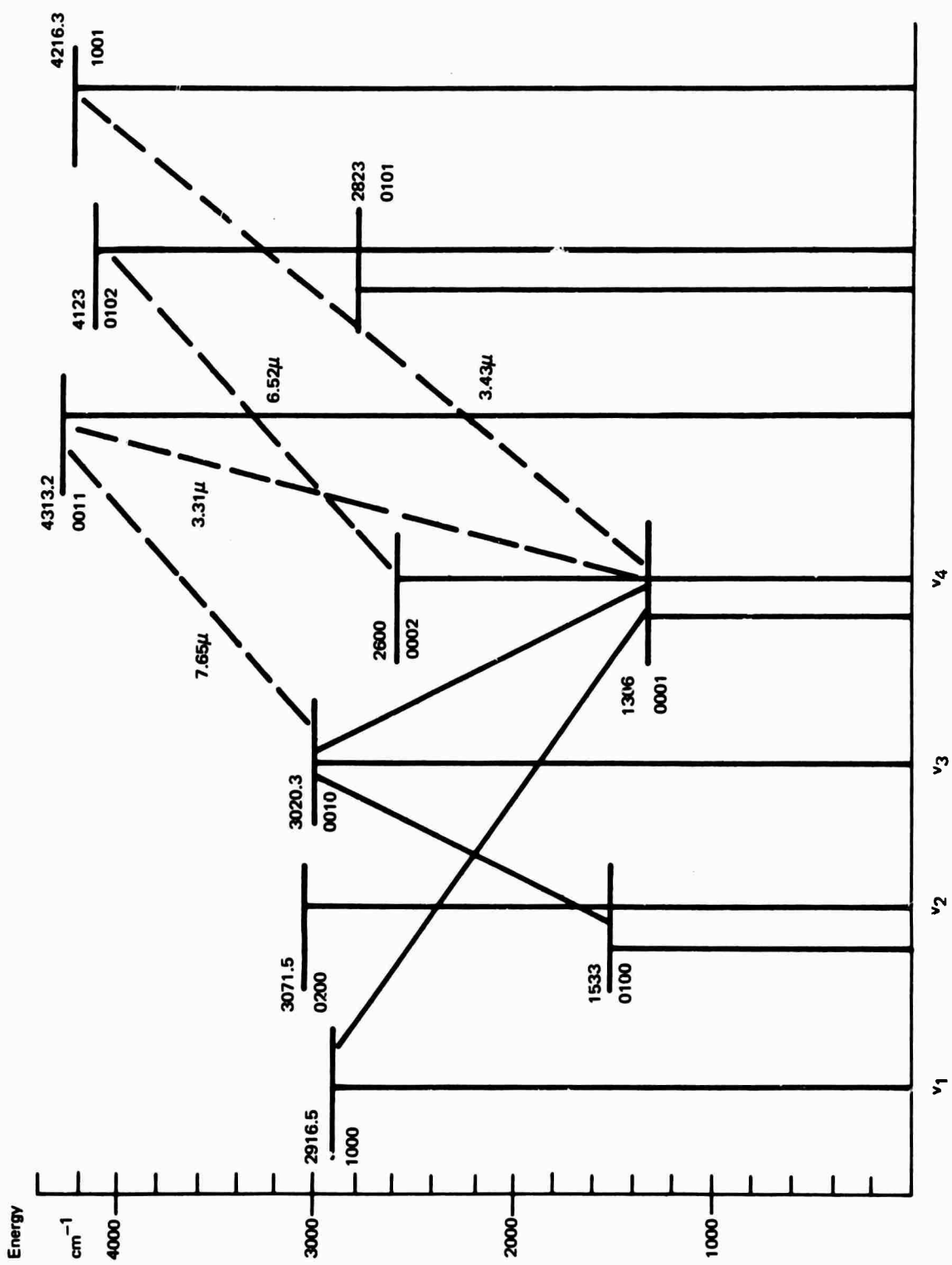


Figure 23. Vibrational Energy Level Diagram of Methane

Table 7. Possible Vibrational Transitions in Methane - CH₄

<u>VIBRATIONAL TRANSITION</u>	<u>ENERGY</u>	<u>WAVELENGTH</u>
0011 → 0010	1292.9 cm ⁻¹	7.75 μ
0011 → 0001	3007.0 cm ⁻¹	3.25
0102 → 0002	1523.0 cm ⁻¹	6.57
0102 → 0101	1300.0 cm ⁻¹	7.70
1001 → 1000	1299.8 cm ⁻¹	7.72
1001 → 0001	2910.1 cm ⁻¹	3.42
0110 → 0100	3013.0 cm ⁻¹	3.19
0110 → 0010	1525.7 cm ⁻¹	6.55

Water-H₂O. The water molecule belongs to the point group C_{2v} and has three nondegenerate normal modes. Two of these modes are totally symmetric and the third is asymmetric, and all three are infrared active. The lowest vibrational energy levels are shown in Figure 24, and possible infrared laser transitions are indicated in Table 8. As can be seen from the energy levels, water exhibits the poorest resonance with the v=1 level of H₂ for the molecules discussed here.

The lack of data on vibrational lifetimes and transition probabilities for the normal modes of the polyatomic molecules discussed above along with lack of experimental evidence of vibrational energy transfer from H₂, such as was available in Morgan and Schiff's (14) work on quenching of N₂^{*}(v=1) by both CO₂ and N₂O, reduces the problem to a tedious experimental search.

4.1 EXPERIMENTAL RESULTS WITH GASES OTHER THAN C₂H₂

The plasma tube described in subsection 3.4 was used for all of the experimental work with gases other than acetylene. In each case, mirror alignment was assured by using N₂-CO₂-He in the tube, and the laser was adjusted for maximum average power.

Various mixtures of the gas under test, H₂, and He were tried with no success. Several capacitors were used to vary the discharge parameters, also without success. In summary, no laser action was observed with NH₃, CCH₄ or H₂O.

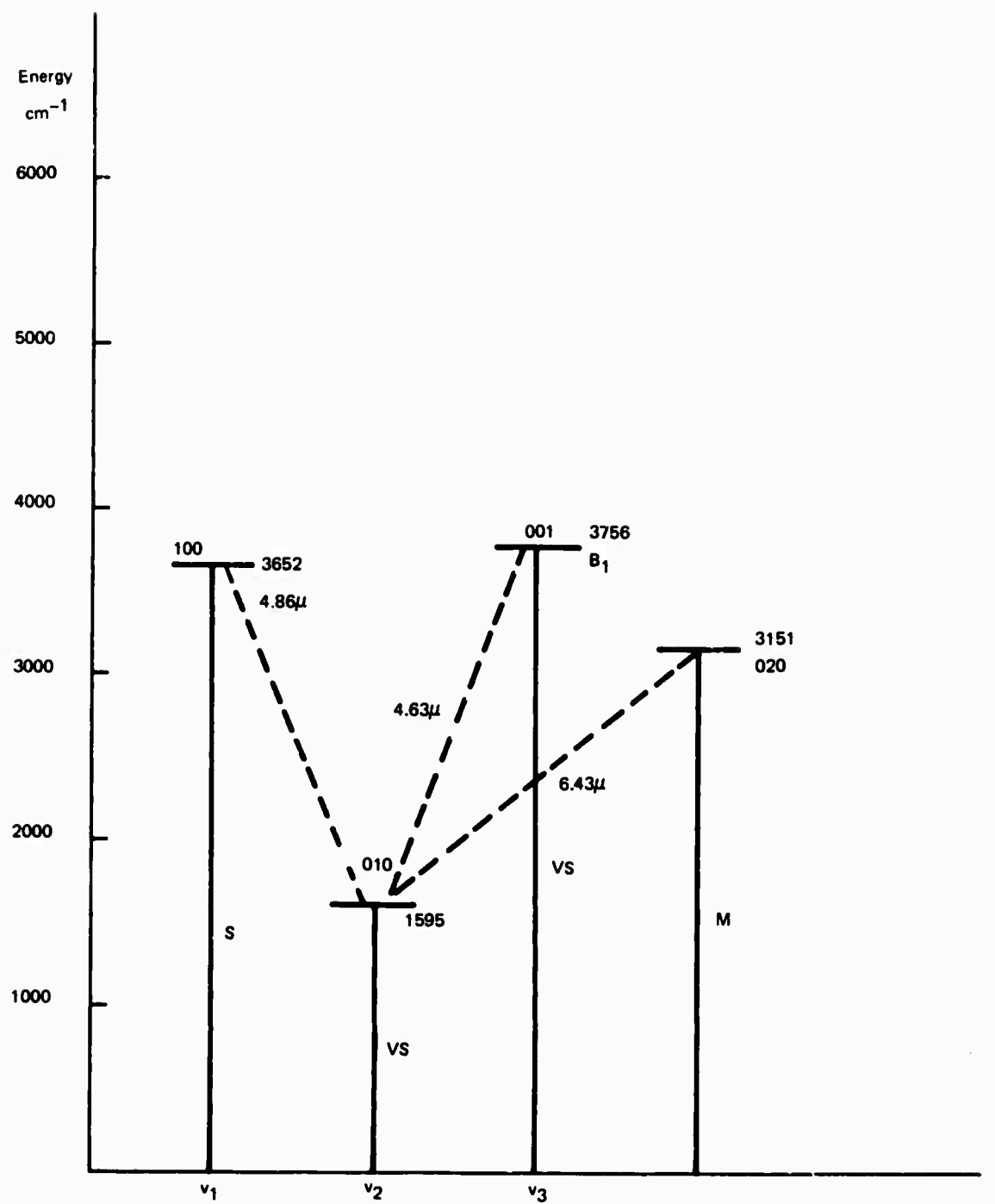


Figure 24. Vibrational Energy Level Diagram of Water Vapor

Table 8. Possible Vibrational Transitions in Water

<u>VIBRATIONAL TRANSITION</u>	<u>ENERGY</u>	<u>WAVELENGTH</u>
$100 \rightarrow 010$	2057 cm^{-1}	4.86 microns
$001 \rightarrow 010$	2161	4.63
$020 \rightarrow 010$	1556	6.43

Section 5. SUMMARY

Before this contract began, laser emission from a flowing mixture of $H_2-C_2H_2-He$ had been discovered in our laboratory. The emission at 8.03 microns was tentatively identified as a Q-branch line of the $\nu_2 - \nu_5^1$ band of the acetylene molecule. The purpose of this program was to study and further characterize the 8.03 micron laser in an effort to determine the importance of resonant energy transfer from vibrationally excited H_2 , and to investigate the possibility of obtaining other laser lines from C_2H_2 in the three to five micron wavelength range. If resonant energy transfer were effective in populating the upper laser level, gases other than acetylene were to be considered.

A total of five lines were observed from the $H_2-C_2H_2-He$ laser at wavelengths of 8.0313, 8.0329, 8.0352, 8.0383, and 8.0416 microns. The lines have been identified as the $J = 5, 7, 9, 11$, and 13 rotational lines in the Q-branch of the $\nu_2 - \nu_5^1$ band in acetylene. Intra- and extra-cavity absorption measurements were used to eliminate spectral lines of discharge products from consideration, and the absorption data also provided an estimate of 2.9 db/meter for the laser gain.

It was also discovered that the acetylene laser could be operated without hydrogen. The absence of hydrogen was most important at high acetylene partial pressures, but at low acetylene pressures the laser output fell less than 25 percent. Acetylene dissociation was monitored by measuring the visible emission from a CH band at 4314Å and a C_2 Swan band at 5165Å. The intensities of these bands increased when hydrogen was removed from the discharge. This implies that less dissociation occurs with hydrogen added. Although there are several possible explanations for this observation, it is likely that the presence of hydrogen prevents the breaking of the triple bond in acetylene by promoting alternative reactions which lead to a retention of acetylene in the lasing volume.

One test for resonant energy transfer from vibrationally excited H_2 was made with a parallel-pumped plasma tube in which an H_2-He discharge took place in one volume and was mixed with C_2H_2 in another. With this arrangement excitation of C_2H_2 cannot come from direct electron excitation, but must take place through collisions with other excited molecules. All attempts to achieve laser emission with this apparatus failed, although simple calculations indicated that deactivating wall collisions could have been responsible.

We did not succeed in obtaining any direct evidence that resonant energy transfer from vibrationally excited H_2 provided a significant contribution to the population of the upper laser level in C_2H_2 . Indications are, however, that direct electron excitation is effective in producing laser emission at 8.03 microns.

NH_3 , CH_4 , and H_2O were substituted for C_2H_2 in the discharge in an effort to find other lasing transitions in the three to five micron range. It was recognized that the probability of success was low without proof of the resonant energy transfer from H_2 , and no laser emission was observed from these gases.

REFERENCES

1. C. F. Shelton, "Vibrational Energy Transfer in Gases Leading to Laser Emission", PhD Thesis, Catholic University of America (1970).
2. V. P. Tychinskii, Soviet Physics Uspekhi, 10, 131 (1967).
3. C. Bradley Moore, et al, J. Chem. Phys., 46, 4222 (1967).
4. C. J. Chen, APS Div. of Electron and Atomic Phys., New York City, Paper Cii (November 1969).
5. N. N. Sobolev and V. V. Sokovikov, Soviet Physics Usphekhi, 10, 153 (1967).
6. W. B. McKnight, J. of Appl. Phys., 40, 2810 (1969).
7. C. K. N. Patel, Phys. Rev., 136, A1187 (1964).
8. F. Legay, et al, Compt. Rend., 260, 3339 (1965).
9. G. Moeller and J. D. Rigden, Appl. Phys. Letters, 7, 274 (1965).
10. C. K. N. Patel, et al, Appl. Phys. Letters, 7, 290 (1965).
11. C. K. N. Patel, SPIE Laser Technology Conference, Rochester, N. Y. (Nov. 1969).
12. C. K. N. Patel, Phys. Rev. Letters, 13, 617 (1964).
13. S. C. Brown, Introduction to Electrical Discharges in Gases, John Wiley & Sons (1966).
14. J. E. Morgan and H. I. Schiff, Can. J. Phys., 41, 903 (1963).
15. C. F. Shelton and F. T. Byrne, Appl. Phys. Letters, 17, 436 (1970).

16. G. Herzberg, Molecular Spectra and Molecular Structure, Vol. II, Infrared and Raman Spectra of Polyatomic Molecules, D. Van Nostrand Company, Inc. (1945).
17. F. L. Keller, "An Evaluation of the Harmonic and Anharmonic Constants of C_2H_2 from a Reinvestigation of its Infrared Spectrum", PhD Thesis, University of Tennessee (1956).
18. R. F. Heidner and J. V. V. Kasper, J. Chem. Phys., 51, 4163 (1969).
19. F. Kaufman and J. R. Kelso, J. Chem. Phys., 28, 510 (1958).
20. F. DeMartini and J. Ducuing, Phys. Rev. Letters, 17, 117 (1966).
21. G. J. Schulz, Phys. Rev., 135, A988 (1964).
22. A. W. Ali and A. D. Anderson, NRL Report No. 6789, "Rate Coefficient Relevant to the H_2 UV Laser" (1969).
23. A. von Engel, Ionized Gases, Oxford Press (1965).
24. G. G. Volpe and F. Zocchi, J. Chem. Phys., 44, 4010 (1967).
25. D. R. Safrany and W. Jaster, J. Phys. Chem., 72, 3305 (1968).
26. E. W. McDaniel, Collision Phenomena in Ionized Gases, John Wiley & Sons, Inc. (1964).
27. E. E. Bell and H. H. Nielsen, J. of Chem. Phys., 18, 1382 (1950).
28. E. E. Bell and H. H. Nielsen, J. of Chem. Phys., 19, 136 (1951).